Escola de Camins
Escola Tècnica Superior d'Enginyeria de Camins, Canals i Ports
UPC BARCELONATECH

Behaviour factors definition for austenitic, duplex and ferritic stainless steel moment resistance frames.

MASTER FINAL THESIS

Final Thesis developed by:
Giovanni Cestari

Directed by:
Esther Real Saladrigas
Isabel González-de-León
Elide Nastri

Master in:
Màster en Enginyeria de Camins, Canals i Ports

Barcelona, January 2023

Department of Civil and Environmental Engineering

Summary

Table Summary

Figure Summary

ADKNOWLEDGE

I thank UPC and UNISA for giving me the opportunity to continue this research work abroad.

I thank the whole UPC steel group particularly Esther Real Saladrigas, Isabel González de León for following me and helping me along the way.

I thank my tutor Elide Nastri present during my university exams and also in this final Chapter.

I thank all the people who have been present in this part of my life.

I dedicate this work to my family, to my mother and father who with many sacrifices have allowed me to study and live unforgettable experiences.

ABSTRACT

The next version of Eurocode 8 greatly modifies the regulations for designing steel Moment Resisting Frames (MRF) in order to promote more efficient and safer designs for seismic loads, and even incorporates a specific Chapter for calculating aluminum systems. However, the next edition does not include a Chapter or specifications for stainless steel structures, despite the considerable differences (greater ductility and strain hardening) that this material presents with respect to other steels.

In this context, the present work investigates the seismic behaviour of stainless steel MRFs designed according to the intermediate ductility classes (DC2) requirements of the new Eurocode 8. The configuration and design of the structures has been based on a study given in literature. Frames with different heights and three stainless steel grades (austenitic, ferritic and duplex) have been analysed.. The force-based approach has been adopted to design the structures, which is based on reducing the seismic action by a calibrated behaviour factor (q). The numerical models have been created by means of the advanced finite element software Abaqus and different analyses of have been performed to obtain the data necessary for applying the verifications proposed for carbon steel MRFs to the cases of study. Moreover, pushover analyses (non-linear static analyses) have been carried out to estimate the actual behaviour factors (q) of all MRFs. It was found that, for the studied cases, the behaviour factor values are higher than the values given in Eurocode 8. Finally, the design methodology given in Eurocode was compared to the design obtained using the Theory of Plastic Mechanism Control (TPMC).

The present work is intended to serve as a starting point for further research into the behaviour of stainless steel structures under seismic actions. Future lines of research are to extend the case studies, to validate the data for DC2, and to calibrate behavior factor (q) values for DC3, and all types of structures present in the new Eurocode 8.

1. Introduction

The world is constantly changing, and human beings are called upon to respond to various needs. Like any industry, the construction industry is constantly evolving, finding materials that are increasingly sustainable and innovative.

Even if it is not a recent discovery, stainless steel represents one of the recent groups of engineering materials. The combination of mechanical properties and corrosion resistance make stainless steel a viable substitute for traditional building materials. The main differences of stainless steel compared to carbon steel, referring to it's structural behaviour, is the non-linear stress-strain relationship and the high ductility, especially for the austenitic ones. Fortunately, research is making great strides studying and understanding the real possibilities of this material.

• 1.1. Objectives

The aim of this research is to study the ultimate behaviour of austenitic, duplex and ferritic moment resistance frames (MRFs) - according to DC2 requirements given in the new version of the Eurocode 8 and to propose values of behaviour factors that can be applied in the Force-based approach for the efficient seismic design of DC2 stainless steel structures.

Finally, an attempt was made to apply an alternative design methodology to the European standards under the name of plastic mechanism theory (TPMC).

• 1.2. Job content

The work is structured in 5 parts and 7 chapters:

1) The state of the art, where stainless steel is introduced, its composition, behaviour, costs, and applications. In this first part, the new revision Eurocode 8 is also introduced, focusing on the aspects related to DC2 that are the subject of this work. And finally, a brief introduction on the behaviour factor and the procedure applied in this research.
2) The case study. Here is a description of the geometry, materials used, profiles, and both vertical and seismic applicated loads.

3) The Chapter concerning the numerical model. Here the finite element software Abaqus utilized in this paper is introduced. In particular, the creation of the model and the various analyses necessary to obtain the data for estimating the behaviour factor values and verification of the structure are explained.
4) The results particularly concerning the significant damage limitation, the second-order effects, the utilisation ratio of members and finally the values of the behaviour factor, are presented in this part.
5) The final part covers the theory of plastic control (TPMC), steps to applicate it, and comparison of results with the Eurocode.

At the end of this document there is the conclusion Chapter where a summary of all the results is made.

2. State of art

- 2.1 Stainless Steel

Stainless steel is an iron-chromium-carbon league, with chromium content of at least 10.5 %, and possible addition of other elements including nickel and molybdenum, are a family of steels resistant to corrosion and high temperatures, properties resulting from the calibration of alloying elements. The high corrosion resistance of stainless steel is possible thanks to the presence of chromium above 10.5 % which allows a natural formation of an adherent and invisible film on the steel surface (DMSSS, 2017).

There are three principal stainless-steel families:

Austenitic Ferritic Duplex

The composition is presented in the following Figures:

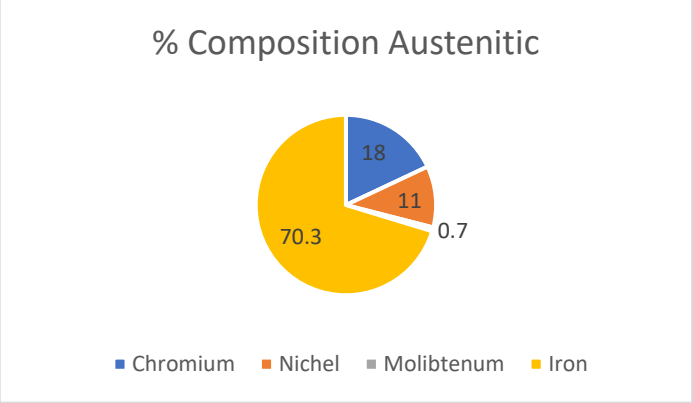

Figure 2. 1 Own production with data source: (DMSSS, 2017)

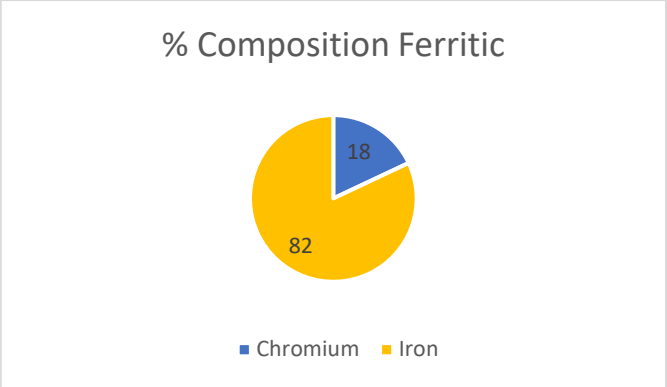

Figure 2. 2 Own production with data source: (DMSSS, 2017)

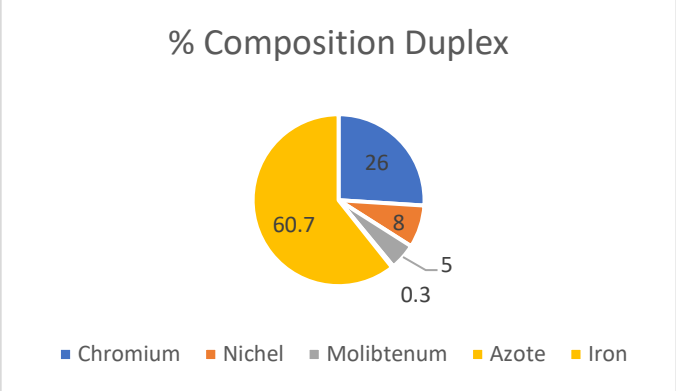

Figure 2. 3 Own production with data source: (DMSSS, 2017)

- *2.1.1 Applications*

Stainless steel can be machined and assembled using a wide variety of processes and techniques and is completely recyclable at the end of its service life. They are the materials of choice for applications in aggressive environments, including buildings and structures in coastal environments exposed to anti-freeze salts and in contaminated locations. The high ductility of stainless steel is a very useful property in seismic applications because it permits greater dissipation of seismic energy.

Even though they are not currently widely used in construction, they are an attractive alternative for applications where mechanical strength and aesthetics matter, in moderately aggressive environments (worldstainless.org).

- *2.1.2 Stress-strain behaviour*

While carbon steel typically exhibits linear elastic behaviour until yield and a plateau before strain hardening is encountered, more rounded response with no definite elasticity limit.

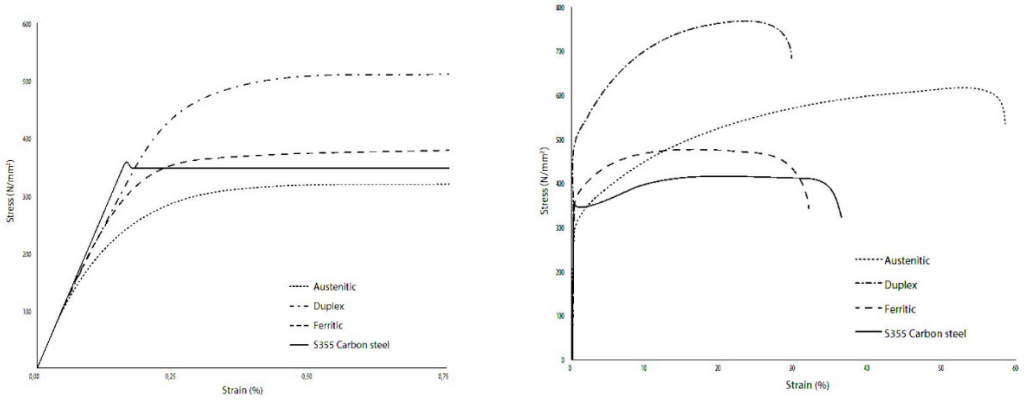

Figure 2. 4 Stress-strain curves for stainless steel and carbon steel from 0 to 0,75 % strain

Figure 2. 5 Full range stress-strain curves for stainless steel and carbon steel

Figure 2.4 compares the stress-strain characteristics of various stainless steels with carbon steels for strains up to 0.75% and Figure 2.5 shows typical stress-strain curves to failure. The yield "limit" of stainless steel is generally referred to as the stress that gives rise to a deviation from the line of proportionality of 0.2 % during the tensile test.

- *2.1.3. Steels comparison of mechanical properties*

Tab.2.1. Mechanical properties of steels: (DMSSS, 2017)

Grade	Strength (N/mm2)	Ductility (%)	Stiffness (N/mm2)
Austenitic Stainless	200 - 240	40	200,000
1.4301 & 1.4307			
1.4401 & 1.4404			
Duplex Stainless	450 - 530	20	200,000
1.4062, 1.4162, 1.4362 etc			
Standard: 1.4462			
Carbon Steel S355	355	22	210,000

Tab.2.1 compares some of the different types of stainless steel and carbon steel.

- *2.1.4. Product standards and strength classes*

The reference standard for stainless steel products is EN 10088. The designation system of EN 10088 is based on the European steel number and the name of the steel.

1	43	07
Denotes steel	Denotes one group of stainless steels	Individual grade identification

X	2	CrNi	18-9
Denotes high alloy steel	100 x % of carbon	Chemical symbols of main alloying elements	% of main alloying elements

- *2.1.5. Costs*

The initial raw material cost of a structural stainless-steel product is higher than of an equivalent carbon steel product, depending on the grade of stainless steel. Considering upfront costs stainless steel seems not to be the cheapest candidate material for structural application. However, there can be initial cost savings associated with eliminating corrosion-resistant coatings. Utilizing high strength stainless steel may reduce material requirements by decreasing section size and overall structure weight which cuts initial costs. Additionally, eliminating the need

for coating maintenance or component replacement due to corrosion can lead to significant long-term maintenance cost savings.

- *2.1.6. Modelling of material behaviour*

The stainless steel material model is based on expression developed by Ramberg and Osgood (1943) and modified: by Hill (1944), by Mirambell and Real (2000), by Rasmussen (2003) and Gardner (2006).

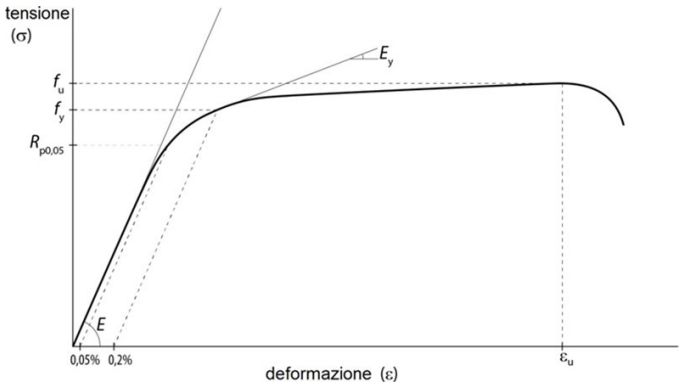

Figure 2.6 Ramberg and Osgood model

The curve shown in Figure 2.6 can be represented by the equations published in (prEN 1993-1-4, 2021).

$$\varepsilon = \frac{\sigma}{E} + 0.002\left[\frac{\sigma}{f_y}\right]^n \qquad \text{per } \sigma \leq f_y$$

(eq.2. 1)

$$\varepsilon = 0.002 + \frac{f_y}{E} + \frac{\sigma - f_y}{E_y} + \left[\frac{\sigma - f_y}{f_u - f_y}\right]^m \qquad \text{per } \sigma \leq f_y$$

(eq.2. 2)

where:

σ: is the engineering stress

ε: is the engineering strain

E: is Elastic modulus

f_y: proof stress and fu ultimate stress

E, f_y, fu: are given in EN 10088

n and m: are parameters calibrated by fitting the experimental curves:

$$m = 1 + 2.8\frac{fy}{fu}$$

(eq.2. 3)

n exponent defines a degree of roundness of the material curve, at low strain. The values of 'n' for each stainless-steel grade and the orientation to the rolling direction defined in the (prEN 1993-1-4, 2021) or calculated with the following formula:

$$n = \frac{\ln(20)}{\ln\left[\frac{f_y}{R_{P0.05}}\right]}$$

(eq.2. 4)

$R_{P0.05}$: is the load value corresponding to a deviation from the proportionality of 0.05%.

E_y: is Secant modulus is the tangent modulus of the stress-strain curve at the yield strength defined as:

$$E_y = \frac{E}{1 + 0.002n[\frac{E}{f_y}]}$$

(eq.2. 5)

ε_u: is the elongation corresponding to the ultimate load, and can be evaluated approximately as follows:

$E_u = 1 - \frac{fy}{fu}$ Austenitic and Duplex

(eq.2.6)

$E_u = 0.6(1 - \frac{fy}{fu})$ Ferritic

(eq.2.7)

- 2.2. European Standards

Eurocode 8, denoted in general by EN 1998: “Design of structures for earthquake resistance”, applies to the design and construction of buildings and civil engineering works in seismic regions.

Eurocode 8 is composed of 6 parts dealing with different types of constructions or subjects:

- EN1998-1: General rules, seismic actions, and rules for buildings
- EN1998-2: Bridges
- EN1998-3: Assessment and retrofitting of buildings
- EN1998-4: Silos, tanks and pipelines
- EN1998-5: Foundations, retaining structures and geotechnical aspects
- EN1998-6: Towers, masts and chimneys

The new Eurocode 8 is also divided in the buildings part alone into two parts:

EN_1998-1-1 (General rules and seismic action) and EN 1998-1-2 (General rules and seismic action).

Code modifications of interest to the following research work include:

- Safety verifications (material overstrength coefficients).
- Introduction of new seismic resistant typology.
- New design concept – new ductility classes.
- Enhancement of the formulation for second order effects.
- Evaluations of lateral displacements.

- *2.2.1. Ductility class*

The new design concept of the Eurocode is structured as follows:

- DC1_Ductility Class 1.
- DC2_Ductility Class 2.
- DC3_Ductility Class 3.

According to (prEN_1998-1-1, 2021) in:

"DC1, the overstrength capacity is taken into account, while the inelastic deformation capacity and energy dissipation capacity are disregarded."

"DC2, the local overstrength capacity, the local deformation capacity and the local energy dissipation capacity are taken into account. Global plastic mechanisms are controlled."

"DC3, the ability of the structure to form a global plastic mechanism at SD limit state and its local overstrength capacity, local deformation capacity and local energy dissipation capacity are taken into account."

Global plastic mechanisms are controlled by limiting drift and second order effects.

DC2 stainless steel structures will be analysed in this study.

- *2.2.2. Capacity design in DC2*

Since DC2 is the ductility class of this research, it will be explored in depth below.

In this part of the standard, unlike in class DC3, where the formulations follow the principles of capacity design, find a few formulations that are intended to prevent the plane collapse mechanism.

The formula in question, also used in the verification in this research is:

$$q_s\, q_r V_{TOT}(q - q_s) d_{e,top} \leq 2 \sum_{i=1}^{n} M_{Rd,c,i}(N_{Ed}) \theta_u^{pl}$$

(eq.2. 8)

It can be seen immediately that eq.2.8 is not a design formula but a verification formula because the first member of the inequation is found $d_{e,top}$.

$d_{e,top}$ is the displacement calculated under the reduced spectrum associated to the design seismic action at the level of the roof top under the design seismic action, which is obtained only after designing the structure.

Analysing the formula again specifically, the second member can be seen to be likened to an internal column work, at the base and head, (of a soft storey), for a plastic rotation. While the first member has the size of a moment because of the product of V_{TOT} and $d_{e,top}$.

The individual components of eq.2.8 are listed below:

- q_S, q_R are reported in Tab.2.2.
- V_{TOT} is the total storey shear in the seismic design situation.
- $d_{e,top}$ is the displacement calculated under the reduced spectrum associated to the design seismic action at the level of the roof top under the design seismic action.
- $M_{Rd.c.i}(N_{Ed})$ is the moment of resistance of column section I where plastic hinge can occur, at the storey under consideration, considering the influence of the axial force N_{ED} in that same section under the gravity load due to masses considered in the seismic analysis of the structure.
- Θ_u^{pl} is the minimum value of the plastic part of the ultimate chord rotation among all the column sections.

Tab.2.2. Individual q terms for carbon steel multistorey moment resisting frames

	q_r	q_s	q_d
DC2	1.3	1.5	1.8

Table 2.2 presents the values of the individual q terms for carbon steel multistorey moment resisting frames. Since there are no values of q for stainless steel frames, carbon steel values were used in this study.

- q_R: is the behaviour factor component accounting for overstrength due to the redistribution of seismic action effects in redundant structures.
- q_S: is the behaviour factor component accounting for overstrength due to all other sources.
- q_D: is the behaviour factor component accounting for the deformation capacity and energy dissipation capacity.

- *2.2.3. Seismic action: response spectrum*

The elastic acceleration response spectrum is a graph that reports, as a function of the natural period of vibration of a building assumed to have indefinitely elastic

behaviour, the maximum acceleration it will experience when it is hit by a seismic event with a given probability of occurrence. By knowing only, the period of vibration of the building and the masses of the decks, it will allow us to estimate the maximum seismic action that the structure should be able to withstand.

According to the revision of the Eurocode 8 (prEN 1998-1-1, 2021), "the seismic design cases should be categorised in seismic action classes depending on the value of the seismic action index, S_δ," defined by the formula:

$$S_\delta = \delta F_\alpha F_T S_{\alpha,475}$$

(eq.2. 9)

The terms of the formula are:

- δ: is a parameter depending on the consequence class of the structure.
- F_α: is the site amplification factor (values can be found in table 5.4 of the normative).
- F_T :is the topographical amplification factor.
- $S_{\alpha,475}$:is spectral acceleration for a return period of 475 years.

Furthermore, new limits have been placed on the selection of ductility classes for design depending on the intensity of seismic action, being DC2 design limited to a seismic action index Sδ not higher than 6.5 m/s2.

In case of designing the structures using the response spectrum method (see Section 2.2.4.), the response spectrum is constructed using the following equations (prEn 1998-1-1, 2021).

$0 \leq T \leq T_A$ $\qquad S_e(T) = \frac{S_\alpha}{F_A}$;

(eq.2. 9)

$T_A \leq T \leq T_B$: $\qquad S_e(T) = \frac{S_\alpha}{T_{B-T_A}}\left[\eta\,(T - T_A) + \frac{T_B - T}{F_A}\right]$;

(eq.2. 10)

$T_B \leq T \leq T_C$: $S_e(T) = \eta S_\alpha$;

(eq.2. 11)

$T_C \leq T \leq T_D$: $S_e(T) = \eta \frac{S_\beta T_\beta}{T}$;

(eq.2. 12)

$T \geq T_D$: $S_e(T) = \eta T_D \frac{S_\beta T_\beta}{T^2}$.

(eq.2. 13)

Where:

- $S_e(T)$: is the elastic response spectrum.
- T: is the vibration period of a linear single-degree-of-freedom system.
- S_α: is the maximum response spectral acceleration (for 5% damping) corresponding to the constant acceleration range of the elastic response spectrum.

$S_\alpha = F_T F_\alpha S_{\alpha, RP}$

(eq.2. 14)

Fα: is the short period site amplification factor

- F_T: is the topography amplification factor.
- $S_{\alpha,RP} = \gamma_{LS,CC} S_{\alpha,ref}$
- S_β: is the 5%-damped response spectral acceleration at the vibration period T_β, given.

$S_\beta = F_T F_\beta S_{\beta,RP}$

(eq.2. 15)

- F_β: is the intermediate period ($T = T_\beta$) site amplification factor.
- $S_{\beta,RP} = \gamma_{LS,CC} S_{\beta,ref}$
- $T_\beta = 1$ s

- T_A is the short-period cut-off associated to the zero-period spectral acceleration.
- F_A is the ratio of Sα to the zero-period spectral acceleration.
- T_C: is the upper corner period of the constant spectral acceleration range.

$$T_C = \frac{S_\beta T_\beta}{S_\propto}$$

(eq.2. 16)

- T_B: is the lower corner period of the constant spectral acceleration range.

$$T_B = \frac{T_C}{\chi} \text{ ; if } 0.05s \leq \frac{T_C}{\chi} \leq 0.10s \text{ ;}$$

(eq.2. 17)

$$T_B = 0.05s \text{ ; if } \frac{T_C}{\chi} < 0.05s \text{ ;}$$

(eq.2. 18)

$$T_B = 0.10s \text{ ; if } \frac{T_C}{\chi} > 0.10s.$$

(eq.2. 19)

- T_D: is the corner period at the beginning of the constant displacement response range of the spectrum.
- η: is the damping correction factor, with a reference value h = 1 for 5% damping ratio.

$$\eta = \sqrt{\left(10 + \frac{T_C(\xi - 5)}{T_C + 30T}\right)/(5 + \xi)}$$

(eq.2. 20)

- ξ: is the damping ratio of the structure, expressed as a percentage of critical.

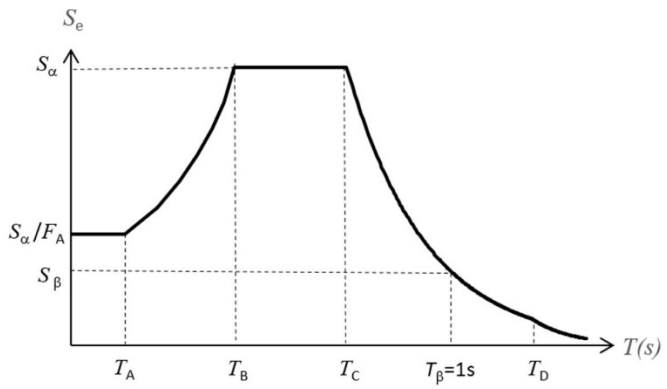

Figure 2.7 Elastic response spectrum shape (with horizontal log scale) (prEN 1998 1-1,2021)

- *2.2.4. Force-based approach*

The force approach, which linear analysis considers the overstrength and the nonlinear response by a behaviour factor q can be implemented with a) or b):

a) the response spectrum method.

b) the lateral force method.

This study used the response spectrum method.

- *2.2.5. Response spectrum method*

Mentioning the standard Eurocode 8 (prEN_1998-1-1, 2021):

"In the force-based approach, in DC1, DC2 or DC3, the seismic action should take the form of a reduced spectrum, derived from the elastic response spectrum by introducing the behaviour factor q, which accounts for overstrength, deformation capacity and energy dissipation capacity".

$$q = q_R q_S q_D$$

(eq.2. 21)

Where the individual terms are represented in the Tab 2.2.

Now we proceed to reduce the spectrum, in each tract, as follows:

$$S_r(T) = \frac{S_e(T)}{R_q(T)} \geq \beta S_{\alpha,475}(T)$$

(eq.2. 22)

where:

$0 \leq T \leq T_A$ $\quad R_q(T) = R_{q0}$

(eq.2. 23)

$T_A \leq T \leq T_B$ $\quad R_q(T) = R_{q0} + \left(q - R_{q0}\right)(T - T_A)/(T_B - T_A)$

(eq.2. 24)

$T_B \leq T$ $\quad R_q(T) = q$

(eq.2. 25)

$$R_{q0} = q_R q_S$$

(eq.2. 26)

And β is the lower bound factor for the horizontal reduced spectrum, equal to 0.08.

- *2.2.6. Control of second order effects*

As mentioned before, global plastic mechanisms are controlled by limiting drift and second order effects.

Mentioning the standard Eurocode 8 (prEN 1998-1-2, 2021):

"Second-order effects (P-Δ effects) may be neglected if the condition given by eq.2.27 is fulfilled in all storeys."

$$\theta \leq 0.10$$

(eq.2. 27)

In DC2 the formula for calculating θ is:

$$\theta = \frac{P_{tot} d_{r,SD}}{\omega_{rm} q_R V_{tot} h}$$

(eq.2. 28)

Valid for moment resisting frames and where:

- P_{tot}: is the total gravity load at and above the storey, due to the masses considered in the seismic analysis of the structure.
- $d_{r,SD:}$ is the horizontal displacement obtained by applying the reduced spectrum.
- V_{tot}: is the total storey shear in the seismic design situation for the force-based approach.
- h: is the inter-storey height.
- $\omega_{rm:}$ is is the material randomness factor accounting for the variability of the steel yield strength in the dissipative zones.

According to Eurocode 8 (prEN 1998-1-2, 2021):

"If $0,1 \leq \theta \leq 0,2$, the second-order effects may approximately be taken into account by multiplying the relevant seismic action effects by a factor equal to $1/ (1 - \theta)$."

"If $0,2 \leq \theta \leq 0,3$ at any storey, the second-order effects should be taken into account directly by using the established methods of second-order analysis which take account of geometric non-linearity, i.e., consider the equilibrium conditions on the deformed structure."

The value of θ should not exceed 0,3.

The value of ωrm depends on the steel grade and is given in Eurocode 8 for carbon steels. This study has assumed the values of ωrm published by Arrayago et al. (2020) for hot rolled section, and given in Table 2.3:

Tab.2.3. Value of ωrm

	Austenitic	Ferritic	Duplex
ωrm	1.22	1.22	1.11

- *2.2.7 Limitation of inter-storey drift*

For the SD Limit state, the inter-storey drift should be limited at any storey of the building by complying with the condition given by Formula (6.3) (prEN 1998-1-2, 2021)

$$d_{r,SD} \leq \lambda_s \, h_s$$

(eq.2. 29)

Where:

- λs: is a coefficient reflecting the limitation of the inter-storey drift.

In general, λs=0.02 for moment resisting frames.

- *2.2.8. Design action for non-dissipative members*

In DC2, the non-dissipative strength of members must be verified against axial N_{Ed}, shear V_{Ed}, and bending forces M_{Ed}, calculated as indicated in the following equations (prEN 1998-1-2, 2021):

$$N_{Ed} = N_{Ed,G} + \Omega N_{Ed,E}$$

(eq.2. 30)

$$M_{Ed} = M_{Ed,G} + M_{Ed,E}$$

(eq.2. 31)

$$V_{Ed} = V_{Ed,G} + V_{Ed,E}$$

(eq.2. 32)

Where:

- $N_{Ed,G}$, $M_{Ed,G}$ and $V_{Ed,G}$ are the actions related to the gravitational combination
- $N_{Ed,E}$, $M_{Ed,E}$ and $V_{Ed,E}$ are the actions related to the seismic combination
- $\Omega = 2$ (for Multi-storey MRFs) is the seismic action magnification factor

• 2.3. Behaviour factor

The behaviour factor is a number denoted by the letter q. This factor has the function of scaling the ordinates of the elastic response spectrum by reducing them, thus giving rise to the design spectrum. The behaviour factor, applied to the elastic response spectrum, defines the resistance that the structure must possess against horizontal actions.

In standards, one can find calibrated values for behaviour factors for carbon steel structures but nothing for stainless steel. Therefore, with this research the effective factor for stainless steel structures will be estimated. There are various methodologies to estimate the structure factor, the one used in this study, and also published in (Lemma et al., 2022) is as follows.

The behaviour factor was estimated through the formula:

$$q = q_{\Omega}\ q_{\xi}\ q_{\mu}\ q_{\rho}$$

(eq.2. 33)

Where:

- q_{ξ}: the factor pertinent to damping.
- q_{Ω}: the over-strength factor (q_r in normative).
- q_{μ}: the ductility factor (q_d in normative).
- q_{ρ}: the over-strength due to all other sources (q_s in normative).

The various factors were estimated through the following equations:

$$q_{\Omega} = \frac{V_y}{V_{1y}}$$

(eq.2. 34)

$$q_{\mu} = \frac{\Delta_u}{\Delta_y}$$

(eq.2. 35)

$$q_{\rho} = \frac{V_{1y}}{V_d}$$

(eq.2. 36)

$$q_{\xi} = 1$$

(eq.2. 37)

The values are obtained through a pushover analysis. Specifically, the points on the curve to be considered are shown in the Figure 2.8 also reported in (Lemma et al., 2022).

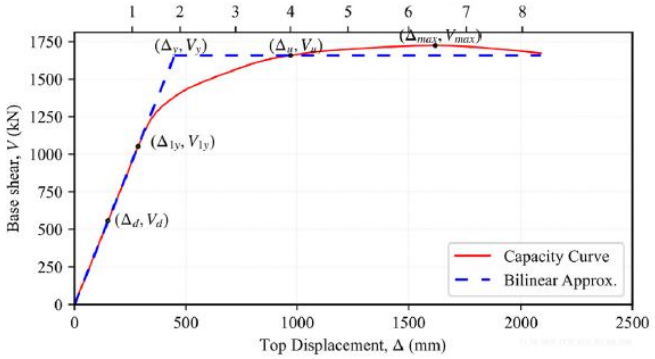

Figure 2.8 Pushover curve bilinear approximation (Lemma et al. 2022)

In Fig. 2.8 it is possible to see an approximation of the pushover curve in terms of displacement and base shear.

The pairs of points are considered as follows:

- (Δ_d;V_d) the design base shear is reached.
- (Δ_{1y};V_{1y}) the first yielding is recorded in any of the elements. It is consider to be reached when the plastic moment is exceeded.
- (Δ_u;V_u) the ultimate limit state has been defined as the least acceleration amplitude where either (1) the columns have buckled, or (2) the maximum inter-storey drift (4%) has been exceeded, or (3) the inelastic deformation capacities of structural members is exceeded and mechanisms form.
- (Δ_{max};V_{max}) the maximum base resistance (base-shear) occurs.
- (Δ_y;V_y) a significant reduction/decline in resistance is registered. The distribution and progression of plastic hinge formations were also monitored.

3. CASE STUDY

In this research the systemic design of moment resisting frames made of stainless steel is studied. The analysed frames coincide with the frames published by Lemma et al. (2022).

They studied how the new revision of Eurocode 8 affected the design and performance of carbon steel frames. In this research, the starting point is the frames designed in carbon steel according to the revised standard by lemma et al. and then see how the design changes using stainless steel profiles.

In this study the influence of height and stainless-steel grade on the behaviour has been analysed. A total of 9 frames have been studied and their results have been compared with the results published in (Lemma et al., 2022).

• 3.1. Geometry description

This study was carried out on frames having the same plan, shown in Figure 3.1, and varying the height and material for each case studied, shown in Figure 3.2,3.3 and 3.4.

As we can see from Figure 3.1 the considered frame has the span width of 6 m, while turning to Figure 3.2, 3.3 and 3.4 it can be seen that floor height remains unchanged and is 3.50 m.

In this study, seismic and gravity forces are resisted by perimeter frames, which are shown in Figure 3.1. It is possible to make assumptions because a fictitious column called leaning column is considered in design and modeling.

The leaning columns are columns with pinned end, supporting gravity loads, which are added to a moment resisting frame or to a braced frame. The column is composed of pendulums because, if it were not so it would have its own stiffness that would affect the stiffness of the frame.

Moreover, in this study, the same initial assumptions that in (Lemma et al., 2022):

- In the other main direction, there is a braced frame that can adequately support design action.

- Means of access to vertical transport, are provided by an independent external structure not covered in this study.
- The columns are assumed to be fixed to the basic level and are continuous over the entire height of the building.
- The beams are assumed to be moment-resisting.
- The seismic mass of the influent is grouped at the nodes.
- The diaphragm action is assumed to model the effect of the floor slab.
- The zone dependent on each peripheral frame in the Y direction is half the zone of the plane adjacent to the frames.

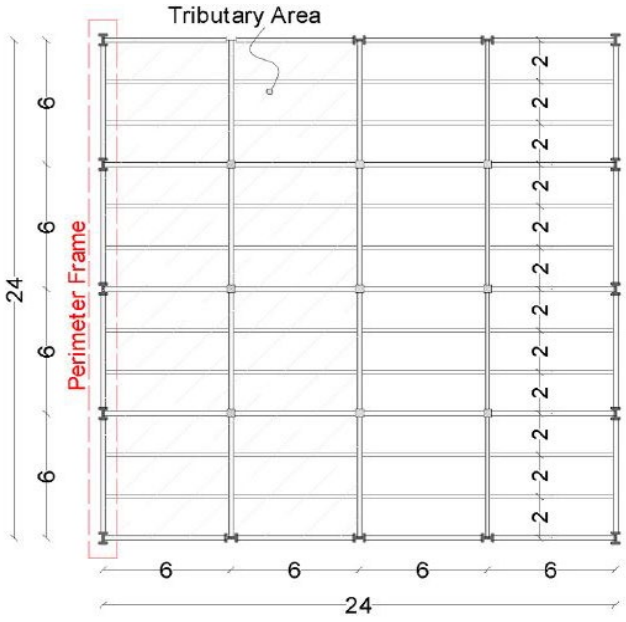

Figure 3.1 Plan. Data source: (Lemma et al., 2022)

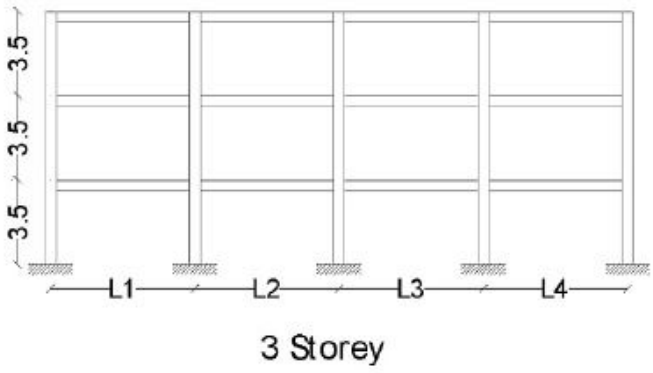

Figure 3.2 Frame 3 storey. Data source: (Lemma et al., 2022)

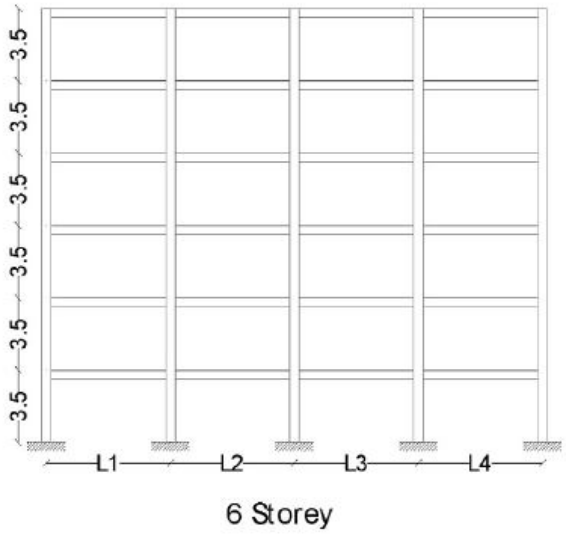

Figure 3.3 Frame 6 storey. Data source: (Lemma et al., 2022)

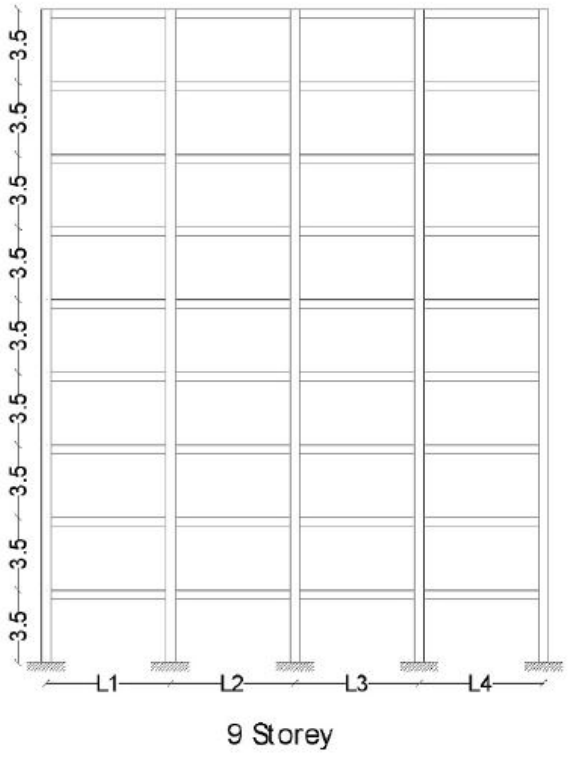

Figure 3.4 Frame 9 storey. Data source: (Lemma et al., 2022)

- 3.2. Materials

As mentioned earlier in this work, stainless steel frames were studied. In particular: Austenitic, Duplex and Ferritic.

Tab.3.1 shows the characteristics of the materials used. Data published in the work of (Afshan et al., 2018) were taken as a reference.

Tab.3. 1 Characteristics of austenitic steels (Afshan et al., 2018)

GRADE	f_y	f_u	ε_u	n	m
Austenitic	280	580	0.50	9.1	2.3
Duplex	530	770	0.30	9.3	3.6
Ferritic	320	480	0.16	17.1	2.8

They were used :

- E = 200000 MPa
- Density = 7.93E-09 $\frac{Kg}{mm^3}$

In this study, the leaning column was modelled with a modulus of elasticity similar to the steel used but with a low density (8.74E-19 $\frac{Kg}{mm^3}$) to make the column not affect the structural response.

- 3.3. Loadings

The gravity loads values are based on those published in (Lemma et al., 2022). In Tab.3.2 the values used.

Tab.3. 2 Loads

Type	kN/m^2
Structural dead load	1.6
Non-structural dead load	1.4
Permanent load gk	3
Live loads qk	3

Tab.3.3 shows the loads considered as concentrated forces on the inner columns, outer columns, and the leaning column. The loads related to the discharges of the secondary beams on the main of the reference frame are also present Fig 3.1.

Tab.3. 3 Vertical loads

Vertical loads							
Fb, conc		Fc, ext		Fc, int		F l, c	
Gk [kN]	Qk [kN]	Gk [kN]	Qk [kN]	Gk [kN]	Qk [kN]	Gk [kN]	Qk [kN]
18	18	9	9	18	18	648	648

Table 3.4 shows the masses used.

Tab.3. 4 Masses

Masses							
Fb, conc		Fc, ext		Fc, int		F l, c	
Gk [Tonnes]	Qk [Tonnes]	Gk [Tonnes]	Qk [Tonnes]	Gk [Tonnes]	Qk [Tonnes]	Gk [Tonnes]	Qk [Tonnes]
1.84	1.84	0.92	0.92	1.84	1.84	66.08	66.08

The following tables show the values of the various load combinations dictated by the standard, namely ULS and SD:

Tab.3. 5 ULS combination

ULS combination			
Fb, conc [kN]	Fc, ext [kN]	Fc, int [kN]	F l, c [kN]
51.3	25.65	51.3	1846.8

Tab.3. 6 SD combination

SD combination			
Fb, conc [kN]	Fc, ext [kN]	Fc, int [kN]	F l, c [kN]
23.4	11.7	23.4	842.4

Tab.3. 7 Punctual Masses

Punctual Masses			
Fb, conc [Tonnes]	Fc, ext [Tonnes]	Fc, int [Tonnes]	F l, c [Tonnes]
2.11	1.06	2.11	75.99

In this study, to account for initial geometric nonlinearities, a system of horizontal forces equivalent to the geometric imperfections was assigned to the frame .

Imperfections can be calculated by a coefficient that is nothing more than a rotation imposed on the frame. This imperfection is calculated by an empirical formula given in the standard (EN 1993-1-1). It can be done in two ways, the first being to give a displacement to the frame of the amount just calculated or to calculate a horizontal stress equivalent to the imperfection.

This stress is equal to:

$$H_{ED} = N_{Ed}\ \varphi$$

(eq.3. 1)

Where:

- H_{Ed}: represents the equivalent horizontal action
- N_{Ed}: represents the total vertical load transferred from the i-th plane
- φ: is the coefficient that accounts for geometric imperfections

$$\Phi = \Phi 0\ \alpha h\ \alpha m$$

(eq.3. 2)

Where:

- φ0: 1/200
- αh: $2/\sqrt{h}$ with h building height in meters
- αm: $\sqrt{0.5(1+1/m)}$ with m equal to the number of columns in a plane

Tab.3.8 and tab.3.9 show the imperfections obtained.

Tab.3. 8 Imperfection ULS

Combo ULS		
Storey	Ned [N]	Hed *φ [N]
Storey 3	2462400	6357.889
Storey 2	2462400	6357.889
Storey 1	2462400	6357.889

Tab.3. 9 Imperfection SD

Combo SD		
Storey	Ned [N]	Hed *φ [N]
Storey 3	1123200	2900.09
Storey 2	1123200	2900.09
Storey 1	1123200	2900.09

- 3.4. Seismic actions

According to (prEN_1998-1-1, 2021), the maximum seismic index allowed for DC2 structures is 6.5. However, since this study adopts the designs proposed by Lemma et al. (2022), the analysis has considered the same seismic action than that considered by Lemma et al (2022), i.e., a seismic index= 7.9

Tab.3. 10 Input Data spectrum.

δ	1		S_δ	7.90	
T_{ref}	475	years	T_A	0.02	[s]
$\gamma_{LS,CC}$	1		T_β	1	[s]
f_h	0.4		χ	4	
$S_{\alpha,ref}$	6.5	[m/s^2]	T_C	0.50	[s]
$S_{\beta,ref}$	2.60	[m/s^2]	T_B	0.10	[s]
$S_{\alpha,475}$	6.5	[m/s^2]	T_D	3.60	[s]
$S_{\alpha,RP}$	6.5	[m/s^2]	T_E	6	[s]
$S_{\beta,RP}$	2.60	[m/s^2]	T_F	10	[s]
F_α	1.22		η	1	
F_β	1.52		β	0.08	
F_T	1		$\beta \cdot S_{\alpha,475}$	0.52	
F_A	2.5				
S_α	7.90				
S_β	3.94				

Tab.3.10 shows all the parameters used for computing the spectrum and applying eq. 2.9 to eq.2.26 is constructed reduced spectrum with and without lower bound as shown in the Figure 3.5 and Figure 3.6.

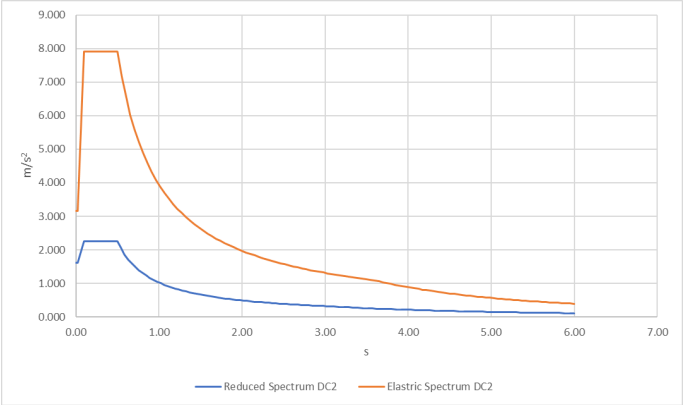

Figure 3. 5 Spectrum DC2 without lb

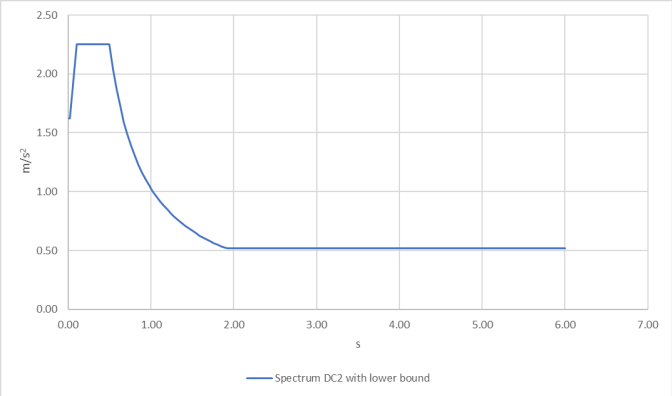

Figure 3. 6 Spectrum DC2 with lb

- 3.5. Profiles

Profiles present in the work of (Lemma et al., 2022) as a starting point and because they were designed with the revised version of the Eurocode i.e., the same one used in this research. The only difference will be the material that in the work of (Lemma et al., 2022) is carbon steel while Stainless steel was used in the present work.

The next tables will show the various profiles for 3, 6 and 9 story frames.

Tab.3.11 Profiles 3-storey frames

Storey	Beams	Ext, col	Int, col
1	IPE 330	HEB 240	HEB 400
2	IPE 330	HEB 240	HEB 360
3	IPE 270	HEB 240	HEB 320

Tab.3. 12 Profiles 6-storey frames

Storey	Beams	Ext, col	Int, col
1	IPE 400	HEB 280	HEB 400
2	IPE 400	HEB 280	HEB 400
3	IPE 360	HEB 280	HEB 400
4	IPE 360	HEB 280	HEB 360
5	IPE 300	HEB 280	HEB 360
6	IPE 300	HEB 280	HEB 360

Tab.3. 13 Profiles 9-storey frames

Storey	Beams	Ext, col	Int, col
1	IPE 400	HEB 320	HEM 400
2	IPE 400	HEB 320	HEM 400
3	IPE 400	HEB 320	HEM 400
4	IPE 400	HEB 280	HEM 400
5	IPE 400	HEB 280	HEM 400
6	IPE 400	HEB 280	HEM 400
7	IPE 360	HEB 240	HEM 400
8	IPE 360	HEB 240	HEM 400
9	IPE 360	HEB 240	HEM 400

4. Numerical model

The analyses carried out in this study were performed using the Abaqus (Systèmes, Dassault, 2011). This Chapter describes the numerical model and in particular: type of elements, geometry, mesh, constraints, materials, loadings, profiles, response spectrum and types of analysis.

• 4.1. Beam elements

The elements used for the modelling of the frames were beam-type elements (B21). The first letter of the name indicates the type of element, in this case "Beam". The next letter indicates the dimensions, which can be 2 in the plane or 3 in the space, The third and last term refer to the type of function, being 1 for linear function, 2 for quadratic function and 3 for cubic. Therefore, in this case in this case were used beam type elements, in the plane and of linear function.

• 4.2. Geometry

This part shows how the data in chapter 3.1 were reported in Abaqus (Systèmes, Dassault, 2011). The part module is used to create the sketch. In this study the sketch was made in a single part because working in 2D it is not necessary to define each element separately and then join them at the end. Important for proper modelling is the definition of sets. In fact, the creation of sets allowed, in this study, to be able to change all the characteristics of each element depending on the exegesis. In this study each element in the sketch has its own sets (e.g. First floor beams, First floor interior columns, etc.…).

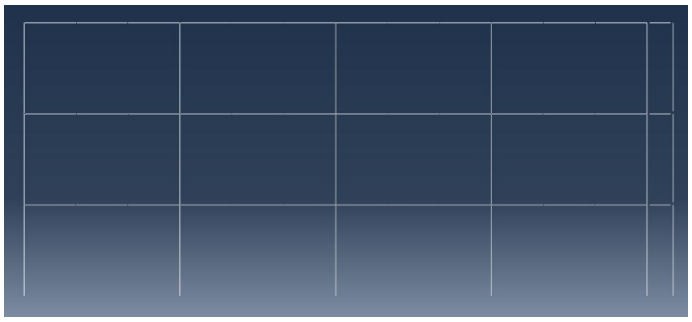

Figure 4. 1 Sketch for a 3-story frame.

Figure 4.1 shows the 2D drawing, in this case of the three-story tarp. You can also see that a column has been drawn on the right with other horizontal elements designed to connect it to the frame. This column is the leaning column described earlier in chapter 3.1. Later Chapters explain how this column should be modelled to comply its function.

- 4.3. Materials

This part explains how the material characteristics introduced in Chapter 3.2 are applied to the model. The power of Abaqus (Systèmes, Dassault, 2011) is that it allows you to set any type of material and thus allow for multiple different analyses.

To assign a material in Abaqus you must first define it. In this case study, austenitic, duplex, and ferritic steels were used for the frames and a different material for the leaning column (described later in this chapter).

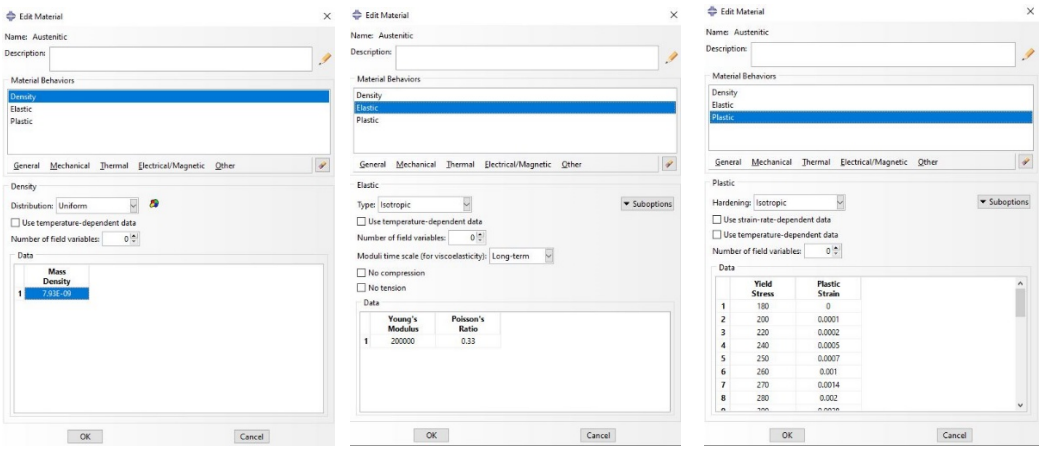

Figure 4. 2 Material definition in Abaqus

Figure 4.2 shows the material definition in Abaqus (Systèmes, Dassault, 2011), in this case of the frame steel. The density, elasticity and plasticity characteristics of the material are then defined as described in Chapter 3.2 and Chapter 2.1.6 specifically with equations 2.1 and 2.2.

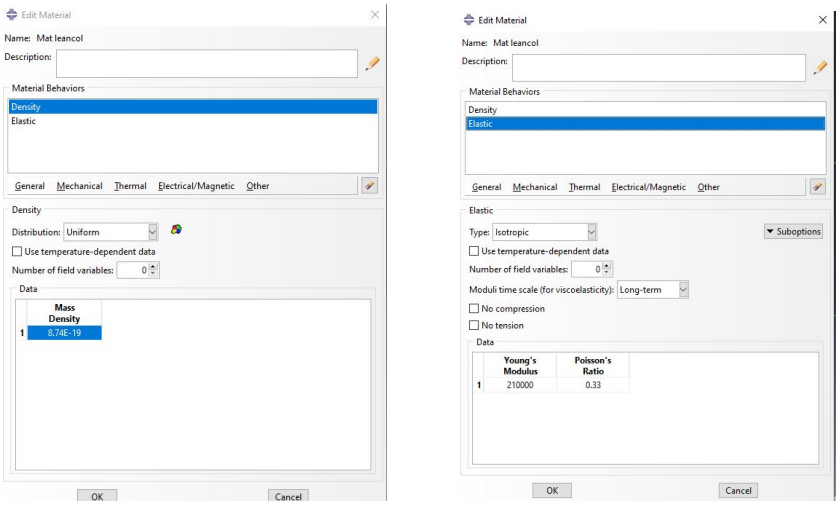

Figure 4. 3 Material definition leaning column.

As can be seen from Figure 4.3, the material of the leaning column was defined in the following way specifically with such a low density (8.74E-19 $\frac{Kg}{mm^3}$) to make the column not affect the structural response.

- 4.4. Profiles and sections

The profiles given in Chapter 3.5 particularly in Tab. 3.11, 3.12 and 3.13, are loaded manually into the program. Very important is the definition of the profile of the leaning column. In this study, the following was modelled with a box-section profile of 1000 mm length for size, so that they have great inertia, to perform its function.

Having defined the various sets in the sketch phase, it was then very easy to associate the profiles and materials to each element.

- 4.5. Mesh

A mesh is an abstraction, a model, whose purpose is not to simulate the outward appearance of a structure, but to simulate the structure's response to the application of certain actions, within the framework of a certain theory, the smaller the mesh the more accurate the results will be. A mesh of 50 mm length elements was created for this study case.

- 4.6. Constraints

Continuing with the modelling of the structure, there is a need to insert constraints to simulate the proper functioning of the model as closely as possible to reality. Have been inserted new sets to facilitate the placement of constraints and loads, and inserted, in the "Engineering Features", the springs to connect the leaning columns to the structure.

Here the constraints needed to simulate the diaphragm are defined. Constraints of the coupling kinematic type are included.

"Kinematic coupling constrains the motion of the coupling nodes to the rigid body motion of the reference node. The constraint can be applied to user-specified degrees of freedom at the coupling nodes with respect to the global or a local coordinate system." (Systèmes, Dassault, 2011)

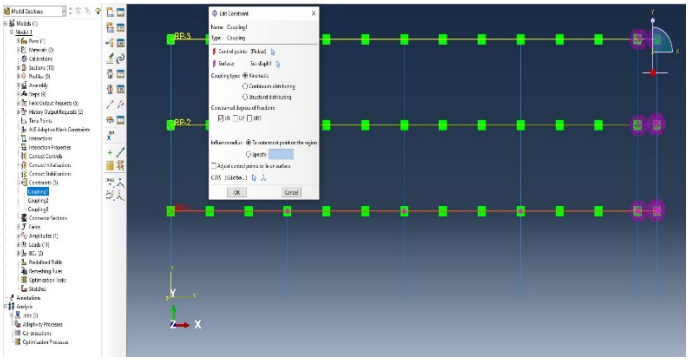

Figure 4. 4 Kinematic coupling constrains.

Figure 4.4 depicts the insertion of the above constraints.

As mentioned before, the leaning column, modelled (i.e., defining material and sections), should be connected to the frame so as not to transmit moments.

It is possible to simulate this scenario with the inclusion of spring-type constraints that lock in the desired degrees of freedom. Figures 4.5 and 4.6 show the insertion of the springs.

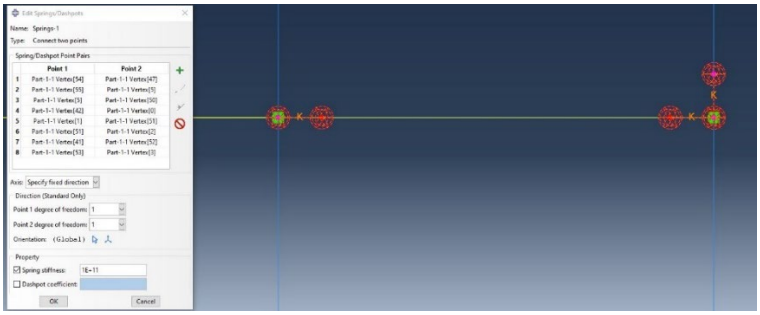

Figure 4. 5 Springs in Abaqus

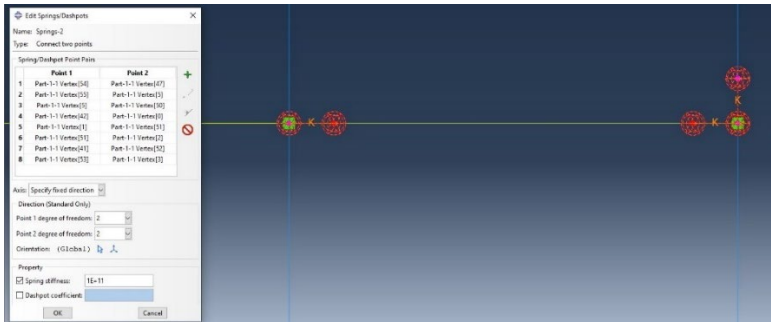

Figure 4. 6 Springs in Abaqus

- 4.7. Loadings

The loads applied to the structure are mentioned in Chapter 3.3. In this case study have been used the following units: (N) and (mm).

In Abaqus (Systèmes, Dassault, 2011), the spectrum should be entered in terms of increasing acceleration (mm/s2), frequency and damping. The data to be entered are the same as those found in Chapter 3.4.

- 4.8. Types of analysis

This research work, as mentioned before, aims at estimating the actual behaviour factors regarding austenitic steel. This work is not thought to design but to verify that the frames with the profiles and materials used are reliable. To do this, the analyses that are performed in Abaqus are as follows:

- Buckle, to find the factor, α_{cr}, and understand whether our structure is suitable.

- Frequency, to find the frequency and period of the first mode of vibration of the structure.
- Spectrum, where the response spectrum is loaded.
- Pushover, allowed us to analyze the data for the calculation of the q factor.

- *4.8.1 Buckle*

Since these are steel structures, it is very important to consider the so-called second-order effects by means of an appropriate buckling analysis. First, the load combination for which to carry out such an analysis is defined:

$$1.35\ G_k + 1.5\ Q_k$$

(eq.4. 1)

Since it is a frame with displaceable nodes even under vertical loads alone, it becomes unstable, so these effects must be taken into account. Specifically, (EN 1993-1-1) requires structures to have at least a first-mode relative buckling coefficient of 3. The standard (EC3) requires, if the coefficient is between 3 and 10 to account for the effects of the second by means of an amplification factor defined as follows:

$$kamp, mod = \frac{1}{1 - \left(\frac{1}{\alpha_{cr,mod}}\right)}$$

(eq.4. 2)

$$\alpha_{cr,mod} = \frac{Ks}{k}\ Y\alpha_{cr}$$

(eq.4. 3)

Eq.4.3 is the modified factor, determined by which the design load would have to be increased to cause elastic instability in a global (sway) mode to account for the influence of plasticity on the sway stiffness of frame. (prEN 1993-1-4, 2021)

Where:

- $\frac{Ks}{k}$: is the ratio of the secant lateral stiffness at the design value of the loading on the structure Fd to the initial lateral stiffness of the structure due to the influence of plasticity (i.e. as obtained from a first order plastic (hinge or zone) analysis. (prEN 1993-1-4, 2021)
- Y: is the factor that approximates the further loss of stiffness due to second order effects. (prEN 1993-1-4, 2021)
- α_{cr} : may be calculated according to Formula (7.2) of (EN 1993-1-1). (prEN 1993-1-4, 2021)

In this study case, being of difficult to estimate $\alpha_{cr,mod}$ is calculated roughly with a coefficient of 0.55 for austenitic, 0.60 for ferritic and 0.65 for duplex that goes to multiply the factor α_{cr} that comes out of the Abaqus buckle analysis, because for the given vertical loading the structure remains in its linear elastic range so $\frac{Ks}{k} = 1$.

This amplification factor goes from amplifying horizontal actions of whatever nature they are.

In this study, to account for initial geometric non-linearities, a system of horizontal forces equivalent to the geometric imperfections tab.3.8 was assigned to the frame.

With the imperfection the loads combo is:

$$ULS\ imperfection \rightarrow \ 1.35\ G_k + 1.5\ Q_k + kamp, mod\ Imperfection$$

(eq.4. 4)

- *4.8.2 Spectral*

The reference linear analysis method for determining the effects of seismic action on both dissipative and non-dissipative systems is modal analysis with response spectrum. Therefore, in order to perform a modal analysis, it is necessary to define additional load combinations, i.e., seismic, for each individual ductility class (in this study case DC2):

$$seismic\ forces\ with\ imperfections\ G_k + 0.3Q_k + E_{DC2,LB} + Imperfection_{SD}$$

(eq.4. 5)

$$seismic\ displacements\ with\ imperfections\ G_k + 0.3Q_k + E_{DC2} + Imperfection_{SD}$$

(eq.4. 6)

Where: $E_{DC2,LB}$ and E_{DC2} are the seismic actions resulting from the application of the spectrum with data in Chapter 3.4.

- *4.8.3 Pushover*

Pushover analysis is a non-linear static analysis method to study the structural behaviour of system under seismic action. This analysis is employed to estimate the resistant capacity of structures implying a dynamic response. In this analysis, the shape of the horizontal load pattern, which aims at simulating dynamic response, can be assumed as constant.

"Lateral forces for pushover analysis should be defined for each horizontal direction of seismic action and their direction should be that of the considered direction of seismic action. The normalized lateral force in the direction under consideration applied at the i-th node of this load pattern should be defined by eq.4.7." (prEN_1998-1-1, 2021)

$$Fi = mi\ \Phi i$$

(eq.4. 7)

Where:

- mi is the mass of the i-th node.
- Φi is the displacement value of mode $\boldsymbol{\Phi}$ at the i-th node in the considered direction of seismic.

5. Results

This Chapter shows the results obtained by applying the verifications given in the code (prEN 1998-1-2, 2021) (see Chapter 2.2) on the analysed frames.

• 5.1. Significant damage limitation – Interstorey drift

The results organized by changing the height and keeping the material constant are shown in Table 5.1, 5.2, 5.3. It should be noted that the change of material does not affect in the performance regarding interstorey drift because with the applied loads the frames remain in the elastic range which remains unchanged for austenitic, duplex and ferritic.

It can be seen from the Tables 5.1, 5.2 and 5.3 that the frames designed with the profiles seen in the Chapter 3.5 as the height changes are verified at the significant damage limit state.

Taking into account the 2% limitation of the legislation, Tab. 5.4 shows that an action could be taken in changing the profiles because in the 3-storey, in the 6-storey case and in the 9-storey case SD_{ur} are lower than the limit, while for the cases reported by Lemma et al. (2022) the interstorey drift is the governing requirement, giving percentages very close to 1% (i.e., drifts close to 70 mm). That is because this study has taken the profiles published in (Lemma et al., 2022), which were calculated considering carbon steel's Young`s modulus, as the final designs for stainless steels.

Table 5. 1 Significant damage limitation for 3-storey frames (regardless the stainless steel grade)

SIGNIFICANT DAMAGE LIMITATION		
STOREY	dr,SD mm	Limit mm
Storey 1	37.915	70
Storey 2	63.303	70
Storey 3	60.450	70

Table 5. 2 Significant damage limitation for 6-storey frames (regardless the stainless steel grade)

SIGNIFICANT DAMAGE LIMITATION		
STOREY	dr,SD mm	Limit mm
Storey 1	36.616	70
Storey 2	57.470	70
Storey 3	57.876	70
Storey 4	54.254	70
Storey 5	38.578	70
Storey 6	20.826	70

Table 5. 3 Significant damage limitation for 9-storey frames (regardless the stainless steel grade)

SIGNIFICANT DAMAGE LIMITATION		
STOREY	dr,SD mm	Limit mm
Storey 1	30.093	70
Storey 2	53.932	70
Storey 3	56.497	70
Storey 4	53.860	70
Storey 5	48.219	70
Storey 6	42.165	70
Storey 7	38.078	70
Storey 8	32.060	70
Storey 9	23.471	70

Table 5. 4 Interstorey drifts for the Significant damage limit state comparison to the 2% limit

	3-storey	6-storey	9-storey
SD ur	0.90 %	0.83 %	0.81 %

- 5.2. Second order effects

The results of the second order effects are shown in this Chapter. The frames designed in this way are all verified and compliant with the standard. It is noted that second-order effects affect more as height increases and duplex stainless steel frames are the most affected by second order effects. This is because in the eq. 2.28 comes into play ω_{rm} that for austenitic and ferritic type stainless steel assumes a value of 1.22 and for duplex assumes a value of 1.11.

Tab.5.8, 5.8.1, 5.12 and 5.12.1 compares the values obtained from this study with those published in (Lemma et al., 2022). As shown, values for carbon steel are lower. It should be noted, that for S355 carbon steel (Lemma et al., 2022) $\omega_{rm} = 1.25$. Moreover, the greater stiffness exhibited by carbon steel frames means that MRFs made on this steel support a higher value of total storey shear force (V_{tot}) than those made on stainless steel. As expected, stainless steel is more sensible to second-order effects.

- *5.2.1 Austenitic and Ferritic stainless steel*

The Tables 5.5, 5.6 and 5.7 show the values of the interstorey-drift sensitivity index θ obtained for the studied frames. As can be seen, the values do not exceed the value of 0.3 dictated by the standard. however, some values exceed 0.1. In this case the standard says to amplify the seismic effects by a coefficient equal to:

$$Factor\ amplitude = \frac{1}{(1-\theta)}$$

(eq.5 1)

Table 5.5 Second order effect 3-storey frames for austenitic and ferritic cases

SECOND-ORDER EFFECTS	
STOREY	ϑ
Storey 1	0.056
Storey 2	0.078
Storey 3	0.052

Table 5.6 Second order effect 6-storey frames for austenitic and ferritic cases

SECOND-ORDER EFFECTS	
STOREY	ϑ
Storey 1	0.118
Storey 2	0.172
Storey 3	0.161
Storey 4	0.126
Storey 5	0.068
Storey 6	0.027

Table 5. 7 Second order effect 9-storey frames for austenitic and ferritic cases

SECOND-ORDER EFFECTS	
STOREY	ϑ
Storey 1	0.104
Storey 2	0.172
Storey 3	0.174
Storey 4	0.154
Storey 5	0.126
Storey 6	0.101
Storey 7	0.081
Storey 8	0.056
Storey 9	0.031

Table 5. 8 Θ max for austenitic and ferritic MRFs

Austenitic and Ferritic	3-storey	6-storey	9-storey
Θ max	0.078	0.172	0.174

Table 5. 8.1 Θ max (Lemma et al., 2022) MRFs

S355	3-storey	6-storey	9-storey
Θ max	0.074	0.107	0.166

- *5.2.2 Duplex stainless steel*

The Tables 5.9, 5.10 and 5.11 show the values of the interstorey-drift sensitivity index θ obtained for the studied frames. As can be seen, the values do not exceed the value of 0.3 dictated by the standard. However, some values exceed 0.1. In these cases, the standard says to amplify the seismic effects by a coefficient equal to eq.5.1.

Table 5. 9 Second order effect index for duplex 3-storey frame

SECOND-ORDER EFFECTS	
STOREY	ϑ
Storey 1	0.069
Storey 2	0.092
Storey 3	0.071

Table 5. 10 Second order effect index for duplex 6-storey frame

SECOND-ORDER EFFECTS	
STOREY	ϑ
Storey 1	0.127
Storey 2	0.186
Storey 3	0.174
Storey 4	0.136
Storey 5	0.074
Storey 6	0.029

Table 5. 11 Second order effects index for duplex 9-storey frame

SECOND-ORDER EFFECTS	
STOREY	ϑ
Storey 1	0.114
Storey 2	0.192
Storey 3	0.189
Storey 4	0.168
Storey 5	0.138
Storey 6	0.110
Storey 7	0.088
Storey 8	0.062
Storey 9	0.034

Table 5. 12 Θ max for duplex MRFs

Duplex	3-storey	6-storey	9-storey
Θ max	0.092	0.186	0.192

Table 5. 12.1 Θ max (Lemma et al., 2022) MRFs

S355	3-storey	6-storey	9-storey
Θ max	0.074	0.107	0.166

- 5.2.3 Utilisation ratio of members

Utilisation ratios are calculated by applying the strength verification formulas proposed in the Design Manual for Structural Stainless Steel (DMSSS, 2017) and the Eurocode 3 (prEN 1993-1-4, 2021).

Tables 5.13- 5.17 show the maximum values concerning the most stressed columns and beams for the austenitic, ferritic and duplex stainless steel frames. Results for reference MRFs are shown in Table 5.16. It is noted that the Ur values for stainless steel MRFs are low due to several causes:

- the design is governed by the interstorey drift, so the profiles are very compact.
- The profiles are not optimized for stainless steels because the same profiles given in (Lemma et al., 2022) for S355 carbon steel are assumed in this study. This explained that duplex stainless steel members are the less optimised because they exhibit a very large f_y compared to those exhibited by the austenitic, ferritic and S355 carbon steel.

Table 5. 13 Utilisation ratio austenitic frames MRFs

Austenitic	$Ur_{,b,max}$	$Ur_{,c,max}$
3-storey	0.49	0.33
6-storey	0.38	0.18
9-storey	0.64	0.32

Table 5. 14 Utilisation ratio duplex frames MRFs

Duplex	$Ur_{,b,max}$	$Ur_{,c,max}$
3-storey	0.26	0.18
6-storey	0.38	0.18
9-storey	0.63	0.31

Table 5. 15 Utilisation ratio ferritic frames MRFs

Ferritic	$Ur_{,b,max}$	$Ur_{,c,max}$
3-storey	0.43	0.29
6-storey	0.34	0.17
9-storey	0.56	0.29

Table 5. 16 Utilisation ratio (Lemma et al., 2022) MRFs

S355	$Ur_{,b,max}$	$Ur_{,c,max}$
3-storey	0.81	0.38
6-storey	0.79	0.42
9-storey	0.92	0.57

6. Behaviour factor

The design of the frames described and verified in the previous Chapters is based on the behaviour factor related to carbon steel due to the lack of data related to stainless steels in the standards. In this Chapter the real behaviour factors q for the studied frames are computed. For this estimation, it is considered the proposal published in (Lemma et al., 2022) and summarised in the eq. 2.33, 2.34, 2.35, 2.36 and 2.37 in Chapter 2.3. To obtain the values of the resistance and drifts that are used in these equations, it was necessary to perform a pushover analysis. The pushover analysis is divided into two parts:

- a first part where the structure is loaded for vertical loads.
- a second part after following the deformation occurred for vertical loads, horizontal loads are added distributed as a function of the fundamental period and amplified until collapse. The ultimate limit state has been defined as the columns have buckled, or the maximum inter-storey drift (4%) has been exceeded (Lemma et al., 2022).

The obtained pushover curves are shown in Chapter 6.1, while the actual values of the behaviour factors are reported in Chapter 6.2.

• 6.1. Pushover curves

Fig. 6.1 to Fig. 6.9 show the pushover responses for the 3-6-9 storey MRFs made on austenitic, duplex and ferritic stainless steel, respectively. The points highlighted in the Figures correspond to those plotted in Fig. 2.8 and needed for computing the behavior factors, i.e., (Δd;Vd), (Δ1y;V1y), (Δy;Vy), (Δu;Vu) (see Chapter 2.3).The ultimate limit state has been defined as the least acceleration amplitude where either (1) the columns have buckled (Δu;Vu), and (2) the maximum inter-storey drift (4%) has been exceeded in the graph represented with (Δu4%;Vu4%)

- *6.1.1 Austenitic MRFs*

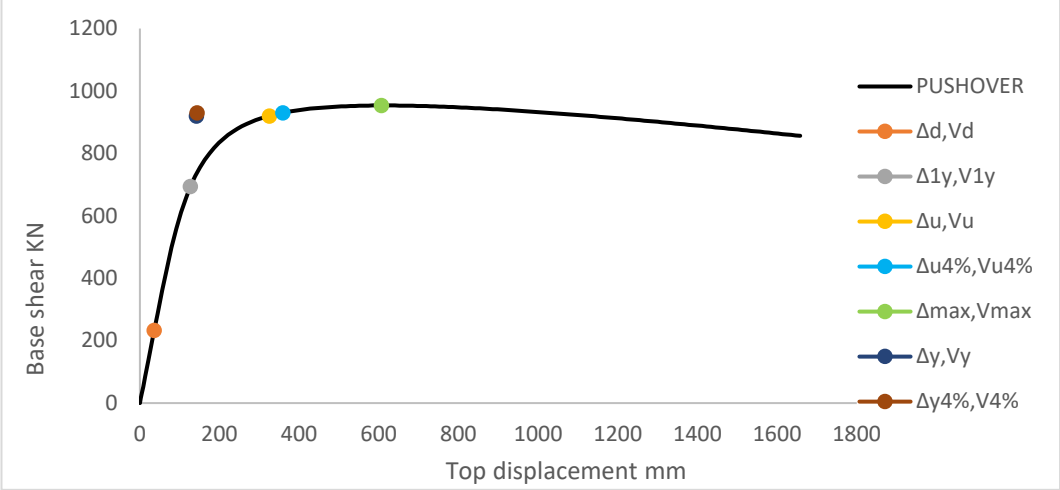

Figure 6. 1 Pushover Austenitic stainless steel 3-s MRFs

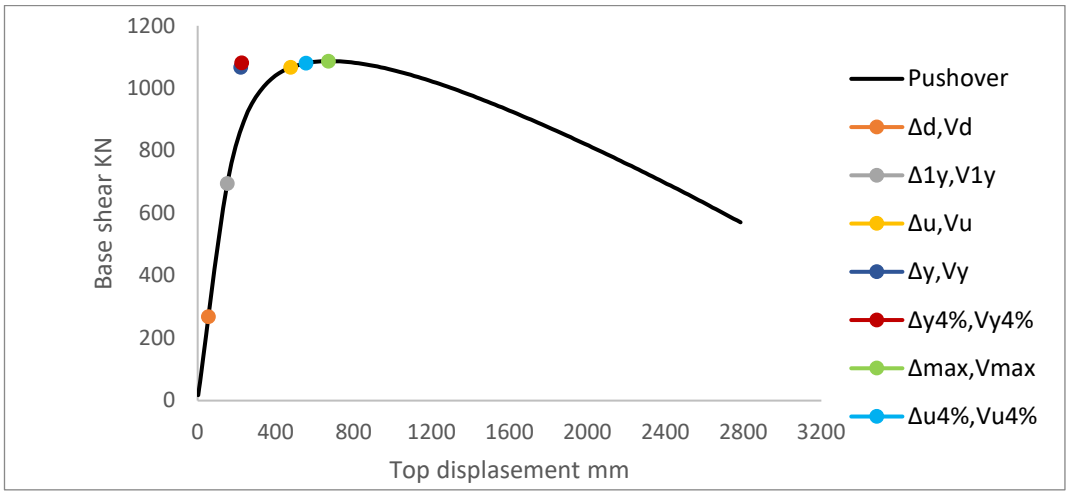

Figure 6. 2 Pushover Austenitic stainless steel 6-s MRFs

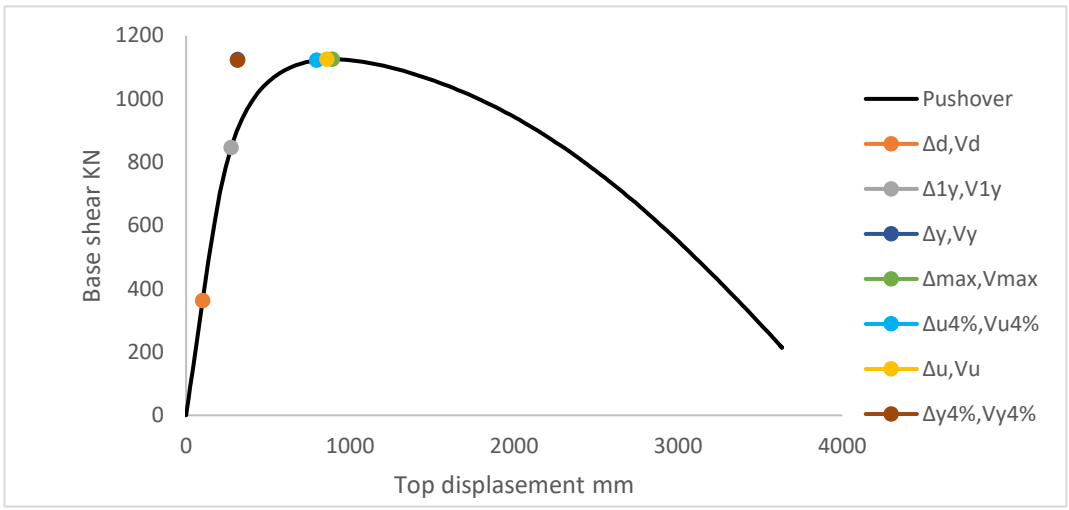

Figure 6. 3 Pushover Austenitic stainless steel 9-s MRFs

- *6.1.2 Ferritic MRFs*

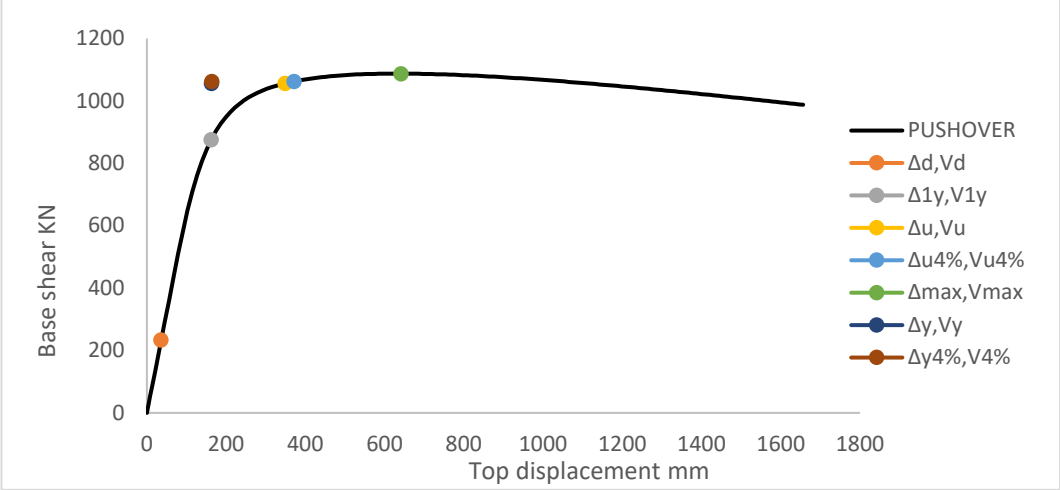

Figure 6. 4 Pushover Ferritic stainless steel 3-s MRFs

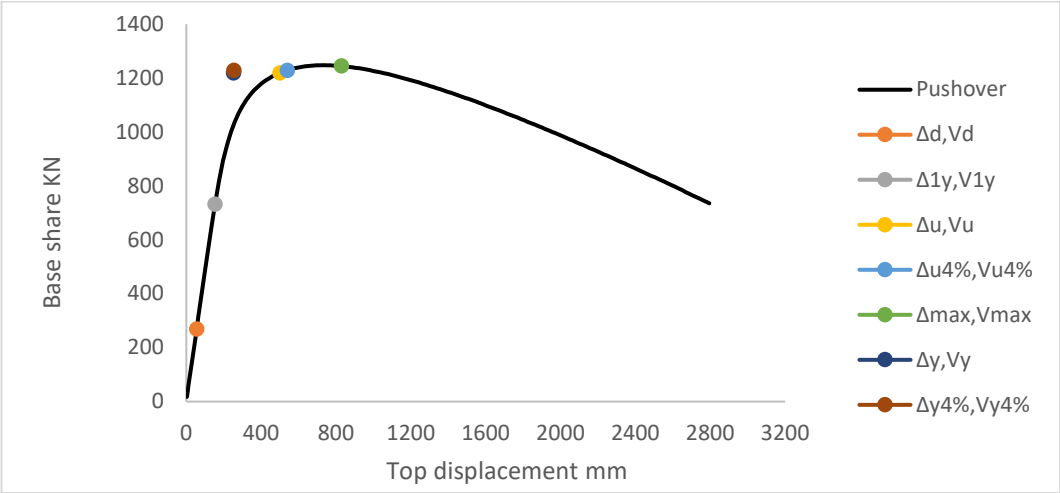

Figure 6. 5 Pushover Ferritic stainless steel 6-s MRFs

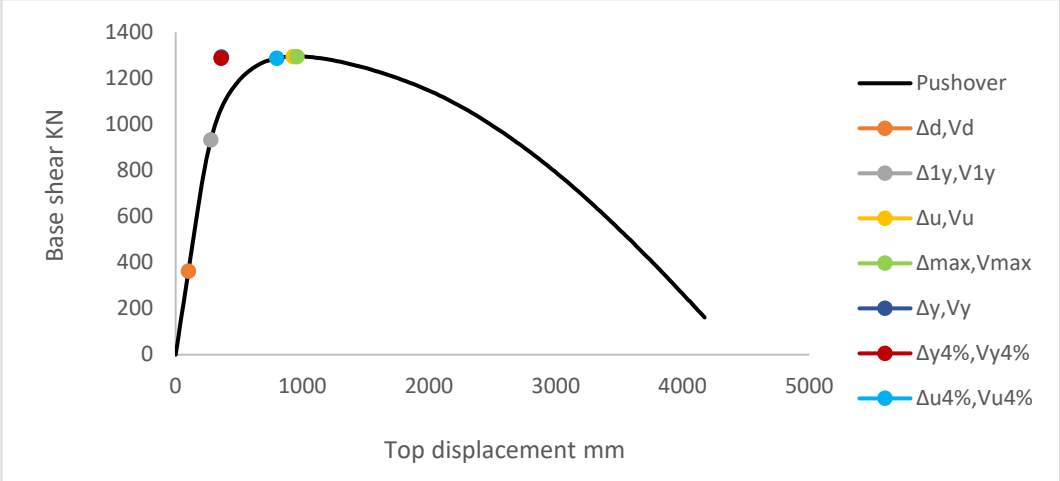

Figure 6. 6 Pushover Ferritic stainless steel 9-s MRFs

- *6.1.3 Duplex MRFs*

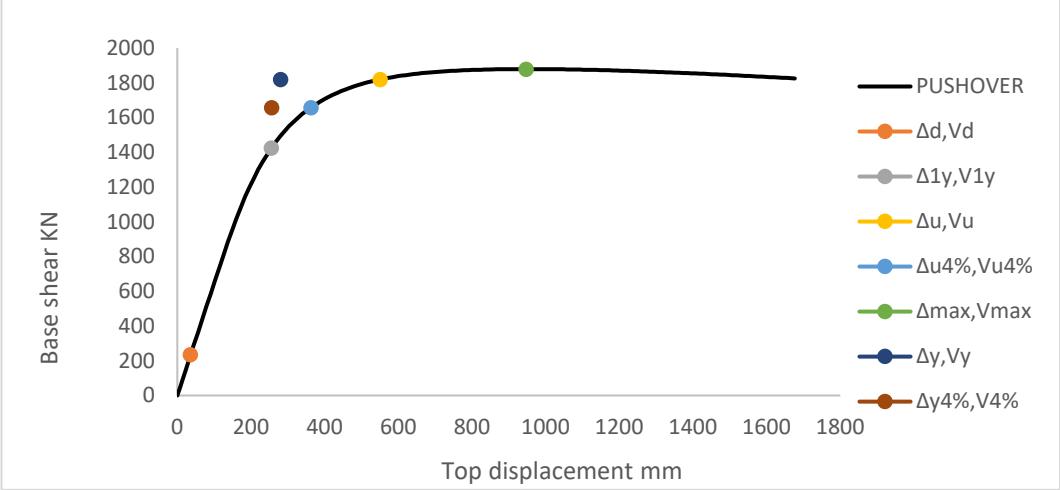

Figure 6. 7 Pushover Duplex stainless steel 3-s MRFs

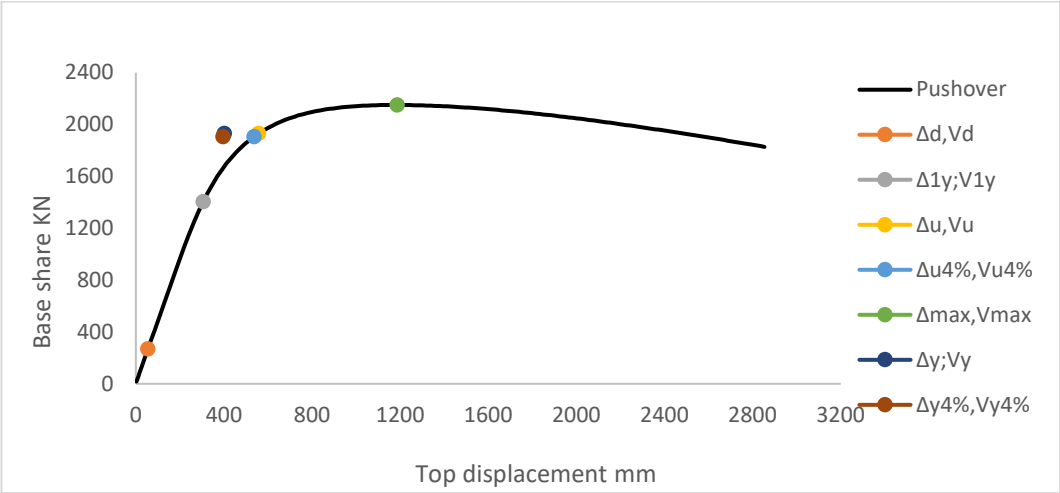

Figure 6. 8 Pushover Duplex stainless steel 6-s MRFs

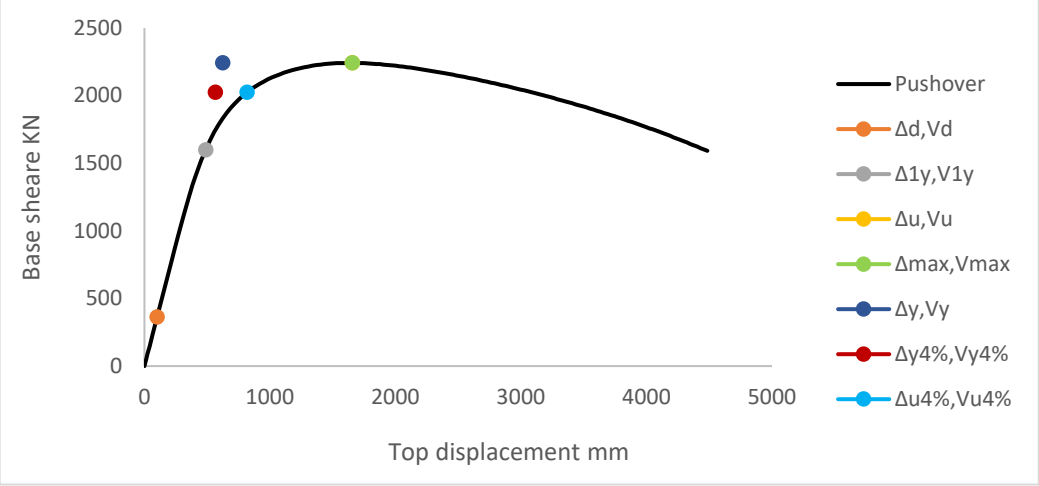

Figure 6. 9 Pushover Duplex stainless steel 9-s MRFs

- 6.2. Behaviour factor values.

Tab.6.1, 6.2 and 6.3 show the behaviour factor values for austenitic, ferritic and duplex MRFs, respectively, considering the ultimate limit state when (1) the columns have buckled and (2) the 4% drift is exceeded. The actual limit state, i.e., the consideration that was reached earlier, has been marked in bold for each case study. The values given by prEN1998-1-2 (2022) are also given for comparison purposes.

As shown in the Tables, the values of the overall performance factor are too high, much higher than the value prescribed by Eurocode (=3.5). This can be explained by the fact that the design of the frames is not optimised for stainless steel.

Focusing on the individual performance factors, the qΩ factor assumes almost the same value in all cases, which is very similar to the value given in the Eurocode (=1.3). It should be noted that the qΩ factor depends on the typology and that the Eurocode does not propose different values depending on the steel grade. Since the case studies are regular multi-storey moment resisting frames (MRFs), it is logical that qΩ assumes a value close to 1.3. The highest values for the qΩ factor are found in 6-storey ferritic MRFs, because in this case V_{1y} is reached much earlier than V_u. Although the austenitic alloy presented a lower yield strength value than the ferritic stainless steel (i.e. the plastic moment is reached a little earlier in the austenitic members), the ferritic frames reached a higher Vu value because their behaviour is less affected by non-linearities.

On the other hand, the actual values of the qμ and qρ factors show a large variability. As can be observed, the highest values of the qμ factor are obtained in austenitic MRFs, while ferritic frames exhibit the lowest value. This is in line with the characteristics of each stainless steel grade, i.e., austenitic stainless steel is very ductile and ferritic stainless steel has a stress-strain behaviour similar to the stress-strain behaviour of carbon steel.

The Eurocode proposes a constant value of 1.5 for the factor qρ, which is the factor related to the excess strength due to other sources, mainly oversizing of the elements. As shown in the Tables, for the cases studied, the qρ factors assume values higher than 2.0, which highlights the fact that for all cases the portal frames are not optimised, especially the 3-storey cases where the qρ factors are higher.

Low-rise structures are more prone to suffer from the soft-storey mechanism, so beam and column profiles tend to be oversized. In terms of material, the lowest values correspond to austenitic stainless steel and the highest to duplex stainless steel, since, as shown in table 3.1, austenitic stainless steel has the lowest yield strength value and duplex the highest

Tab.6. 1 Comparison behaviour factor as height changes austenitic stainless steel

	Austenitic	qΩ	qξ	qμ	qρ	q
3-s MRFs	Buck.col	**1.33**	**1**	**2.29**	**2.98**	**9.05**
	Drift 4%	1.34	1	2.50	2.98	10.01
6-s MRFs	Buck.col	**1.54**	**1**	**2.16**	**2.59**	**8.57**
	Drift 4%	1.56	1	2.47	2.59	9.92
9-s MRFs	Buck.col	1.33	1	3.04	2.33	9.42
	Drift 4%	**1.32**	**1**	**2.54**	**2.33**	**7.86**
EC8		1.3		1.8	1.5	3.5

Tab.6. 2 Comparison behaviour factor as height changes ferritic stainless steel

	Ferritic	qΩ	qξ	qμ	qρ	q
3-s MRFs	Buck.col	**1.21**	**1**	**2.14**	**3.77**	**9.71**
	Drift 4%	1.21	1	2.26	3.77	10.34
6-s MRFs	Buck.col	**1.66**	**1**	**1.98**	**2.73**	**8.99**
	Drift 4%	1.68	1	2.12	2.73	9.72
9-s MRFs	Buck.col	1.36	1	2.83	2.57	9.88
	Drift 4%	**1.38**	**1**	**2.23**	**2.57**	**7.91**
EC8		1.3		1.8	1.5	3.5

Tab.6. 3 Comparison behaviour factor as height changes duplex stainless steel

	Duplex	qΩ	qξ	qμ	qρ	q
3-s MRFs	Buck.col	1.28	1	1.96	**6.12**	15.34
	Drift 4%	**1.16**	**1**	**1.42**	**6.12**	**10.11**
6-s MRFs	Buck.col	1.37	1	1.39	5.23	10.00
	Drift 4%	**1.36**	**1**	**1.36**	**5.23**	**9.63**
9-s MRFs	Buck.col	1.40	1	2.65	4.41	16.41
	Drift 4%	**1.26**	**1**	**1.45**	**4.41**	**8.11**
EC8		1.3		1.8	1.5	3.5

7. THEORY OF PLASTIC MECHANISM CONTROL

An innovative tool for seismic design of steel structures, is the "Theory of Plastic Mechanism Control" (TPMC) initially proposed by Mazzolani and Piluso, subsequently update by (V. Piluso et al., 2022).

Within the method of hierarchy criteria, it has been widely demonstrated that this criterion is generally able to prevent soft story mechanisms but does not assure the development of a collapse mechanism of global type, unlike the TPMC.

TPMC is based on the kinematic theorem of plastic collapse extended to the concept of collapse mechanism equilibrium curve. The kinematic theorem of plastic collapse asserts that the collapse multiplier is the minimum between all kinematically admissible multipliers. Starting from the assumption of a rigid-plastic behaviour, the attention is focused on the structure collapse state. Moreover, second order effects are directly accounted for by the concept of the collapse mechanism equilibrium curve.

The mechanism equilibrium curve is a straight line which can generally be expressed in the following form where α_0 is the kinematically admissible multiplier of the horizontal forces in accordance with a rigid-plastic analysis of the first order; ψ is the slope of the collapse mechanism equilibrium curve.

$$\boldsymbol{\alpha = \alpha_0 - \psi\theta}$$

(eq.7. 1)

In this new formulation, the ultimate rotation (θu) is used instead of the ultimate displacement (δu).

The design condition assures that the global mechanism equilibrium curve is always below undesired mechanism curve in the boundary of the interval between $\theta=0$ and $\theta=\theta u$ because the slope $\psi(g)$ not always is lower than the slopes associated to the undesired mechanism.

$$\psi^{(g)} = \frac{\sum_{k=1}^{n_s} V_k h_k}{\sum_{k=1}^{n_s} F_k h_k}$$

(eq.7. 2)

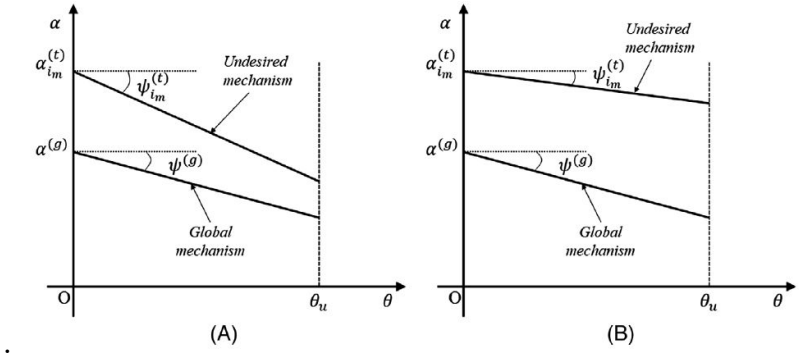

Figure 7.1 Design conditions to avoid undesired mechanisms (A), slope of global mechanism lower than slope of undesired mechanism, (B) slope of global mechanism greater than slope of undesired mechanism) (V. Piluso et al., 2022)

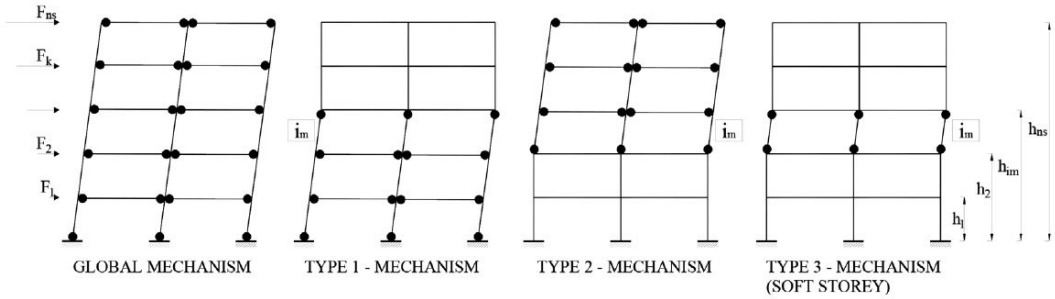

Figure 7. 2 Collapse mechanism of MR-frame

This Chapter aims to apply the method for the studied 6-storey austenitic stainless steel moment resisting frame. Please refer to the article for demonstration and research of the equations used: (V. Piluso et al., 2022)

- 7.1. Closed Form Solution, Columns design.

The following are the steps to follow:

1) Select a design plastic rotation θu, compatible with the ductility supply of structural members.
2) Compute the slopes $\alpha - \theta$ of the mechanism equilibrium curves $\psi_{i_m}^{(t)}$ by the equations:

   Slope of the mechanism equilibrium type 1

$$\psi_{i_m}^{(1)} = \frac{\sum_{k=1}^{i_m} V_k h_k + h_{i_m} \sum_{k=i_m+1}^{n_s} V_k}{\sum_{k=1}^{i_m} F_k h_k + h_{i_m} \sum_{k=i_m+1}^{n_s} F_k}$$

(eq.7. 3)

Slope of the mechanism equilibrium type 2

$$\psi_{i_m}^{(2)} = \frac{\sum_{k=i_m}^{n_s} V_k \left(h_k - h_{i_m-1}\right)}{\sum_{k=i_m}^{n_s} F_k \left(h_k - h_{i_m-1}\right)}$$

(eq.7. 4)

Slope of the mechanism equilibrium type 3

$$\psi_{i_m}^{(3)} = \frac{\sum_{k=i_m}^{n_s} V_k}{\sum_{k=i_m}^{n_s} F_k}$$

(eq.7. 5)

3) Design the beam sections and the first storey columns. The required sum of plastic moment of first storey columns:

$$\sum_{i=1}^{n_c} M_{c.i1} \geq \frac{2 \sum_{k=1}^{n_s} \sum_{j=1}^{n_b} M_{b.jk} + \left(\psi_1^{(t)} - \psi^{(g)}\right) \theta \sum_{k=1}^{n_s} F_k h_k}{2 \frac{\sum_{k=1}^{n_s} F_k h_k}{h_1 \sum_{k=1}^{n_s} F_k} - 1}$$

(eq.7. 6)

$$\sum_{i=1}^{n_c} M_{c.i.1,\max} = \max\left\{\sum_{i=1}^{n_c} M_{c,i1}\,(\theta = 0); \sum_{i=1}^{n_c} M_{c,i1}\,(\theta = \theta_u)\right\}$$

(eq.7. 7)

In particular $M_{(b.jk)}$ is the plastic moment of the beams and n_b indicates the number of bays.

4) Compute the axial load acting in the columns at the collapse state, that is, when a collapse mechanism of global type is completely developed.

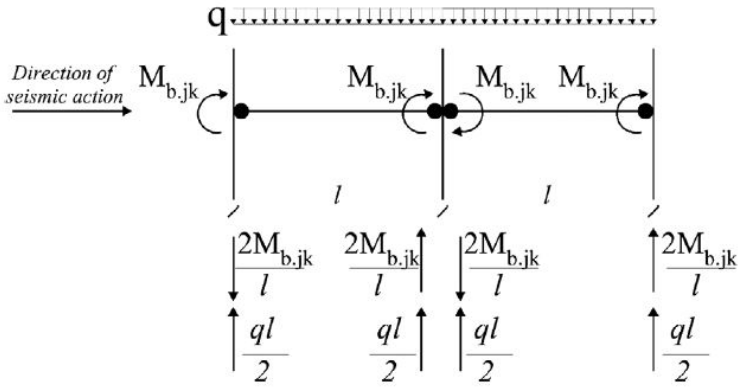

Figure 7.2 Loads transmitted by the beams to the columns at collapse state (V. Piluso et al., 2022)

5) The sum of the plastic moments required on the first storey to avoid the soft-storey mechanism is divided among the columns.
6) The appropriate columns profiles are chosen from the standard shapes so that the plastic moment is greater than that required one. So, it is possible to obtain the effective sum of the plastic moments of the columns at the first storey $\sum_{i=1}^{n_c} M^*_{c.i.1}$ that is used to calculate $\alpha_0^{(g)}$

$$\alpha_0(g) = \frac{\sum_{i=1}^{n_c} M^*_{c.i.1} + 2\sum_{k=1}^{n_s}\sum_{j=1}^{n_b} M_{b.jk}}{\sum_{k=1}^{n_s} F_k\, h_k}$$

(eq.7. 8)

7) Compute the required sum of the plastic moment of columns, reduced due to the contemporary action of the axial force.

$$\sum_{i=1}^{n_c} M^{(1)}_{c.i\ i_m}(0) \geq \alpha_0^{(g)} \left(\sum_{k=1}^{i_m} F_k h_k + h_{i_m} \sum_{k=i_m+1}^{n_s} F_k \right) - \sum_{i=1}^{n_c} M^*_{c.i1} - 2\sum_{k=1}^{i_m-1}\sum_{j=1}^{n_b} M_{b.jk}$$

(eq.7. 9)

$$\sum_{i=1}^{n_c} M^{(2)}_{c.i\ i_m}(0) \geq \alpha_0^{(g)} \sum_{k=i_m}^{n_s} F_k(h_k - h_{i_m-1}) - 2\sum_{k=i_m}^{n_s}\sum_{j=1}^{n_b} M_{b.jk}$$

(eq.7. 10)

$$\sum_{i=1}^{n_c} M_{c.i\ i_m}^{(3)}(0) \geq \alpha_0^{(g)} \left(\frac{h_{i_m} - h_{i_m-1}}{2} \right) \sum_{k=i_m}^{n_s} F_k$$

(eq.7. 11)

$$\sum_{i=1}^{n_c} M_{c.i\ i_m}^{(1)}(\theta_u) \geq \left(\alpha^{(g)} + \psi_{i_m}^{(1)} \theta_u \right) \left(\sum_{k=1}^{i_m} F_k h_k + h_{i_m} \sum_{k=i_m+1}^{n_s} F_k \right) + - \sum_{i=1}^{n_c} M_{c.i1}^{*} - 2 \sum_{k=1}^{i_m-1} \sum_{j=1}^{n_b} M_{b.jk}$$

(eq.7. 12)

$$\sum_{i=1}^{n_c} M_{c.i\ i_m}^{(2)}(\theta_u) \geq \left(\alpha^{(g)} + \psi_{i_m}^{(2)} \theta_u \right) \sum_{k=i_m}^{n_s} F_k (h_k - h_{i_m-1}) - 2 \sum_{k=i_m}^{n_s} \sum_{j=1}^{n_b} M_{b.jk}$$

(eq.7. 13)

$$\sum_{i=1}^{n_c} M_{c.i\ i_m}^{(3)}(\theta_u) \geq \left(\alpha^{(g)} + \psi_{i_m}^{(3)} \theta_u \right) \left(\frac{h_{i_m} - h_{i_m-1}}{2} \right) \sum_{k=i_m}^{n_s} F_k$$

(eq.7. 14)

8) Compute of the required sum of the plastic moments of columns for each storey as the maximum value among those coming from the above design conditions:

$$\sum_{i=1}^{n_c} M_{c.i\ i_m} = max \left\{ \begin{array}{l} \sum_{i=1}^{n_c} M_{c.i\ i_m}^{(1)}(0), \sum_{i=1}^{n_c} M_{c.i\ i_m}^{(1)}(\theta_u), \sum_{i=1}^{n_c} M_{c.i\ i_m}^{(2)}(0), \sum_{i=1}^{n_c} M_{c.i\ i_m}^{(2)}(\theta_u), \\ \sum_{i=1}^{n_c} M_{c.i\ i_m}^{(3)}(0), \sum_{i=1}^{n_c} M_{c.i\ i_m}^{(3)}(\theta_u) \end{array} \right\}$$

(eq.7. 15)

9) Distribute the sum of the required plastic moment at each storey.

If necessary, a technological condition is imposed by requiring, starting from the base, that the column sections cannot increase along the building height. If this condition requires the change of the column sections of the first storey, then the procedure needs to be repeated from step (5).

- 7.2. Case study

The case study is a 6-story frame with austenitic stainless steel.

Tab.7. 1 Input data TPMC

Storey	h_k	L_e	G_k	Q_k	ψ_2	F_{C1}	F_{C2}	F_{Ic}	$q_{d.masse}$	ψ_{Ei}	F_{C1}	F_{C2}	F_{Ic}	Weight
	[m]	[m]	[kN/m^2]	[kN/m^2]	[-]	[kN]	[kN]	[kN]	(kN/m2)	[-]	[kN]	[kN]	[kN]	[kN]
1	3.5	24.0	3.0	3.0	0.3	35.1	70.2	842.4	0	0.3	35.1	70.2	842.4	1123.2
2	7.0	24.0	3.0	3.0	0.3	35.1	70.2	842.4	0	0.3	35.1	70.2	842.4	1123.2
3	10.5	24.0	3.0	3.0	0.3	35.1	70.2	842.4	0	0.3	35.1	70.2	842.4	1123.2
4	14.0	24.0	3.0	3.0	0.3	35.1	70.2	842.4	0	0.3	35.1	70.2	842.4	1123.2
5	17.5	24.0	3.0	3.0	0.3	35.1	70.2	842.4	0	0.3	35.1	70.2	842.4	1123.2
6	21.0	24.0	3.0	3.0	0.3	35.1	70.2	842.4	0	0.3	35.1	70.2	842.4	1123.2

Let's go on to calculate a seismic force distribution. In this case, we consider the same values for T1, and Sa(T1) used previously.

Tab.7. 2 Force distribution

T_1	$S_a(T_1)$	λ	F_d
[s]	[m/s^2]	[-]	[kN]
1.90	0.52	0.85	304.81

Tab.7. 3 Force distribution

Storey	z_i	W_i	$z_i Wi$	F_k
	[m]	[kN]	[kN m]	[kN]
1	3.5	1123.2	3931.2	14.51
2	7.0	1123.2	7862.4	29.03
3	10.5	1123.2	11793.6	43.54
4	14.0	1123.2	15724.8	58.06
5	17.5	1123.2	19656	72.57
6	21.0	1123.2	23587.2	87.09
		6739.2	82555.2	304.81

Selection of a design rotation, θ_u, compatible with the local ductility resources of the structure members. In this case, the value of the plastic rotation resulting from the Eurocode is equal to 0.021 rad.

Using the formulas mentioned above we go on to calculate the slopes of the collapse mechanism equilibrium curves of the undesired mechanisms. The results are shown in Tab 7.5

Tab.7. 4 Slope curves

Storey	$h_{intersotrey}$	h_k	F_k	$F_k h_k$	V_k	$V_k h_k$	Ψ_{im} (1)	Ψ_{im} (2)	Ψ_{im} (3)
	[m]	[m]	[kN]	[kN m]	[kN]	[kN m]	[-]	[-]	[-]
1	3.500	3.500	14.515	50.802	1053.000	3685.50	20.73	16.74	20.73
2	3.500	7.000	29.029	203.206	1053.000	7371.00	19.46	15.55	18.14
3	3.500	10.500	43.544	457.215	1053.000	11056.50	18.44	14.51	16.12
4	3.500	14.000	58.059	812.826	1053.000	14742.00	17.65	13.60	14.51
5	3.500	17.500	72.574	1270.040	1053.000	18427.50	17.07	12.80	13.19
6	3.500	21.000	87.088	1828.858	1053.000	22113.00	16.74	12.09	12.09

The preliminary design of beams can be simply conducted by appropriately estimating the maximum bending moment occurring.

The beams previously used in the design performed according to the codes.

Tab.7. 5 Beams profiles TPMC.

Storey	Profiles
1	IPE 400
2	IPE 400
3	IPE 360
4	IPE 360
5	IPE 300
6	IPE 300

Considering the rigid node, the plastic hinges at the ends of the beams are not formed in the node but translated by a distance 2sh and the plastic moment of the beams will be multiplied by a coefficient equal to

$$coefficient = \frac{l}{l - 2sh}$$

(eq.7. 16)

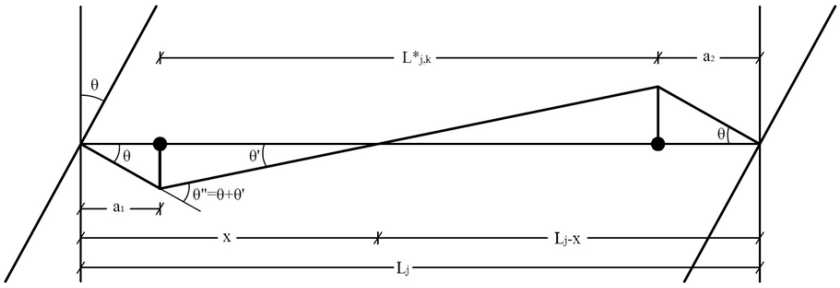

Figure 7.3 Plastic hinge position

Tab.7. 6 Ultimate moments Beams

Mu [kN m]	Storey
5269.82	1
5269.82	2
4108.60	3
4108.60	4
2506.85	5
2506.85	6

The sum of the plastic moments of the columns required on the second floor (reduced due to the simultaneous action of the axial stress) to avert undesired collapse mechanisms, -i=1 Mc.i.1nc, is calculated by means of the relation in step (3).

The axial load acting in the columns in the collapse condition, i.e., when the collapse mechanism of global type is fully developed are reported in Tab. 7.8.

Consequently, the internal design stresses (Mc,i1, N c,i1 for i=1,2,...,nc) are known and the column sections can be designed. Since the column sections are chosen from the book profiles guide. The obtained values of the summation of Mc,i1 are generally larger than the minimum required value. Therefore, the equilibrium curve of the mechanism must be calculated using the latter value.

Storey 1									
columns	Nq [kN]	Nb [kN]	Nc [kN]	Ntot [kN]	ripart	Mc (kNm)	Wpl.req (cm^3)	PROFILE	Wpl.obt (cm^3)
1	0.00	926.50	210.60	1137.10	0.200	630.20	2250.702568	HE 400 B	3232
2	0.00	0.00	421.20	421.20	0.200	630.20	2250.702568	HE 400 B	3232
3	0.00	0.00	421.20	421.20	0.200	630.20	2250.702568	HE 400 B	3232
4	0.00	0.00	421.20	421.20	0.200	630.20	2250.702568	HE 400 B	3232
5	0.00	926.50	210.60	1137.10	0.200	630.20	2250.702568	HE 400 B	3232

Tab.7. 7 Plastic moment summation required columns floor 1

columns	A (cm^2)	N_{Rd} (kN)	n	a	M_{Rd} (kNm)	Check
1	197.8	5538.4	0.20531197	0.27199191	904.96	VERO
2	197.8	5538.4	0.07605085	0.27199191	904.96	VERO
3	197.8	5538.4	0.07605085	0.27199191	904.96	VERO
4	197.8	5538.4	0.07605085	0.27199191	904.96	VERO
5	197.8	5538.4	0.20531197	0.27199191	904.96	VERO
6				**$\Sigma M_{c,i,1}$* [kNm]**	**4524.80**	

In Tab 7.9 the summation of the plastic moments of the columns (reduced due to the simultaneous action of the normal stress) required to avoid the undesired collapse mechanisms with the relations of the point (7) are reported.

Tab.7. 8 Summation of the plastic moments of the columns

Storey	Σ Mci,1(θu)	Σ Mci,2(θu)	Σ Mci,3(θu)	max Σ Mci	Σ Mci(θ=0)	Σ Mci,2(θ=0)	Σ Mci,3(θ=0)
1	4524.80	(-)	4524.80	4524.80	4524.80	(-)	4524.80
2	3072.91	-15325.12	3124.26	3124.26	2953.84	-15235.81	3109.38
3	3388.06	-11034.00	2792.49	3388.06	3280.90	-10914.93	2798.44
4	3907.80	-8401.76	2314.17	3907.80	3836.36	-8294.60	2332.04
5	3177.84	-4812.89	1689.32	3177.84	3148.07	-4741.45	1710.16
6	2506.85	-3177.84	917.93	2506.85	2506.85	-3148.07	932.81

The sum of the plastic moments should be distributed among the columns:

Tab.7. 9 Storey 2 TPMC

Column	Nq [kN]	Nb [kN]	Nc [kN]	Ntot [kN]	ripart	Mc (kNm)	Wpl.req (cm^3)	PROFILE	Wpl.obt (cm^3)
1	0.00	721.56	175.50	897.06	0.200	624.85	2231.617388	HE 400 B	3232
2	0.00	0.00	351.00	351.00	0.200	624.85	2231.617388	HE 400 B	3232
3	0.00	0.00	351.00	351.00	0.200	624.85	2231.617388	HE 400 B	3232
4	0.00	0.00	351.00	351.00	0.200	624.85	2231.617388	HE 400 B	3232
5	0.00	721.56	175.50	897.06	0.200	624.85	2231.617388	HE 400 B	3232
					$\Sigma M_{c,i,2}$* [kNm]	**3124.26**			

Tab.7. 10 Check Storey 2 TPMC

Column	A (cm^2)	N_{Rd} (kN)	n	a	M_{Rd} (kNm)	Check
1	197.8	5538.4	0.16197137	0.27199191	904.96	Verified
2	197.8	5538.4	0.0633757	0.27199191	904.96	Verified
3	197.8	5538.4	0.0633757	0.27199191	904.96	Verified
4	197.8	5538.4	0.0633757	0.27199191	904.96	Verified
5	197.8	5538.4	0.16197137	0.27199191	904.96	Verified

Tab.7. 11 Storey 3 TPMC

Column	Nq [kN]	Nb [kN]	Nc [kN]	Ntot [kN]	ripart	Mc (kNm)	Wpl.req (cm^3)	PROFILE	Wpl.obt (cm^3)
1	0.00	516.62	140.40	657.02	0.200	677.61	2420.043211	HE 400 B	3232
2	0.00	0.00	280.80	280.80	0.200	677.61	2420.043211	HE 400 B	3232
3	0.00	0.00	280.80	280.80	0.200	677.61	2420.043211	HE 400 B	3232
4	0.00	0.00	280.80	280.80	0.200	677.61	2420.043211	HE 400 B	3232
5	0.00	516.62	140.40	657.02	0.200	677.61	2420.043211	HE 400 B	3232
					$\Sigma M_{c,i,3}$* [kNm]	**3388.06**			

Tab.7. 12 Check Storey 3 TPMC

Column	A (cm^2)	N_{Rd} (kN)	n	a	M_{Rd} (kNm)	Check
1	197.8	5538.4	0.11863077	0.27199191	904.96	Verified
2	197.8	5538.4	0.05070056	0.27199191	904.96	Verified
3	197.8	5538.4	0.05070056	0.27199191	904.96	Verified
4	197.8	5538.4	0.05070056	0.27199191	904.96	Verified
5	197.8	5538.4	0.11863077	0.27199191	904.96	Verified

Tab.7. 13 Storey 4 TPMC

Colonna	Nq [kN]	Nb [kN]	Nc [kN]	Ntot [kN]	ripart	Mc (kNm)	Wpl.req (cm^3)	PROFILE	Wpl.obt (cm^3)
1	0.00	356.85	105.30	462.15	0.200	781.56	2791.287418	HE 400 B	3232
2	0.00	0.00	210.60	210.60	0.200	781.56	2791.287418	HE 400 B	3232
3	0.00	0.00	210.60	210.60	0.200	781.56	2791.287418	HE 400 B	3232
4	0.00	0.00	210.60	210.60	0.200	781.56	2791.287418	HE 400 B	3232
5	0.00	356.85	105.30	462.15	0.200	781.56	2791.287418	HE 400 B	3232
					$\Sigma M_{c,i,4}$* [kNm]	**3907.80**			

Tab.7. 14 Check Storey 4 TPMC

Column	A (cm^2)	N_{Rd} (kN)	n	a	M_{Rd} (kNm)	Check
1	197.8	5538.4	0.08344385	0.27199191	904.96	Verified
2	197.8	5538.4	0.03802542	0.27199191	904.96	Verified
3	197.8	5538.4	0.03802542	0.27199191	904.96	Verified
4	197.8	5538.4	0.03802542	0.27199191	904.96	Verified
5	197.8	5538.4	0.08344385	0.27199191	904.96	Verified

Tab.7. 15 Storey 5 TPMC

Colonna	Nq [kN]	Nb [kN]	Nc [kN]	Ntot [kN]	ripart	Mc (kNm)	Wpl.req (cm^3)	PROFILE	Wpl.obt (cm^3)
1	0.00	197.07	70.20	267.27	0.200	635.57	2269.884669	HE 340 B	2408
2	0.00	0.00	140.40	140.40	0.200	635.57	2269.884669	HE 340 B	2408
3	0.00	0.00	140.40	140.40	0.200	635.57	2269.884669	HE 340 B	2408
4	0.00	0.00	140.40	140.40	0.200	635.57	2269.884669	HE 340 B	2408
5	0.00	197.07	70.20	267.27	0.200	635.57	2269.884669	HE 340 B	2408
					$\Sigma M_{c,i,5}$* [kNm]	**3177.84**			

Tab.7. 26 Check Storey 5 TPMC

Column	A (cm^2)	N_{Rd} (kN)	n	a	M_{Rd} (kNm)	Check
1	170.9	4785.2	0.05585268	0.24517262	674.24	Verified
2	170.9	4785.2	0.02934047	0.24517262	674.24	Verified
3	170.9	4785.2	0.02934047	0.24517262	674.24	Verified
4	170.9	4785.2	0.02934047	0.24517262	674.24	Verified
5	170.9	4785.2	0.05585268	0.24517262	674.24	Verified

Tab.7. 37 Storey 6 TPMC

Colonna	Nq [kN]	Nb [kN]	Nc [kN]	Ntot [kN]	ripart	Mc (kNm)	Wpl.req (cm^3)	PROFILE	Wpl.obt (cm^3)
1	0.00	98.53	35.10	133.63	0.200	501.37	1790.606926	HE 300 B	1869
2	0.00	0.00	70.20	70.20	0.200	501.37	1790.606926	HE 300 B	1869
3	0.00	0.00	70.20	70.20	0.200	501.37	1790.606926	HE 300 B	1869
4	0.00	0.00	70.20	70.20	0.200	501.37	1790.606926	HE 300 B	1869
5	0.00	98.53	35.10	133.63	0.200	501.37	1790.606926	HE 300 B	1869
					Σ $M_{c,i,6}$* [kNm]	**2506.85**			

Tab.7. 48 Check Storey 6 TPMC

Column	A (cm^2)	N_{Rd} (kN)	n	a	M_{Rd} (kNm)	Check
1	149.1	4174.8	0.03200947	0.23541247	523.32	Verified
2	149.1	4174.8	0.01681518	0.23541247	523.32	Verified
3	149.1	4174.8	0.01681518	0.23541247	523.32	Verified
4	149.1	4174.8	0.01681518	0.23541247	523.32	Verified
5	149.1	4174.8	0.03200947	0.23541247	523.32	Verified

If necessary, a technological condition is imposed in that, starting from the base, the column sections cannot increase along the height of the building.

If the fulfilment of this condition requires increasing the column sections on the second floor, the procedure needs to be repeated.

By distributing the classical moment equally among all the columns, the profiles obtained are:

Tab.7. 19 Profiles columns TPMC

Storey	Profiles
1	HEB 400
2	HEB 400
3	HEB 400
4	HEB 400
5	HEB 340
6	HEB 300

- *7.2.1 Validation of the procedure by means of push-over analysis.*

To evaluate the seismic performance of the designed structures, analyses were performed using the Abaqus computer program. The purpose of these analyses is to evaluate the type of collapse mechanisms to confirm the accuracy of the proposed design methodologies based on the new prEN1998 standards and the Theory of Control of Plastic Mechanisms. In Figure 7.4 it is possible to see how the pushover curve stays below the curve representing the global collapse mechanism, up to a limit rotation. So, it is possible to say in this way the soft plane mechanism and the other types of mechanisms are avoided. As Figure 7.1 also shows. With this procedure relying on the kinematic theorem of plastic collapse extended to the concept of collapse mechanism equilibrium curve and a simple spreadsheet, it is possible to obtain an initial conformal sizing with the ideal of averting unwanted collapse mechanisms and designing a structure with a collapse global mechanism.

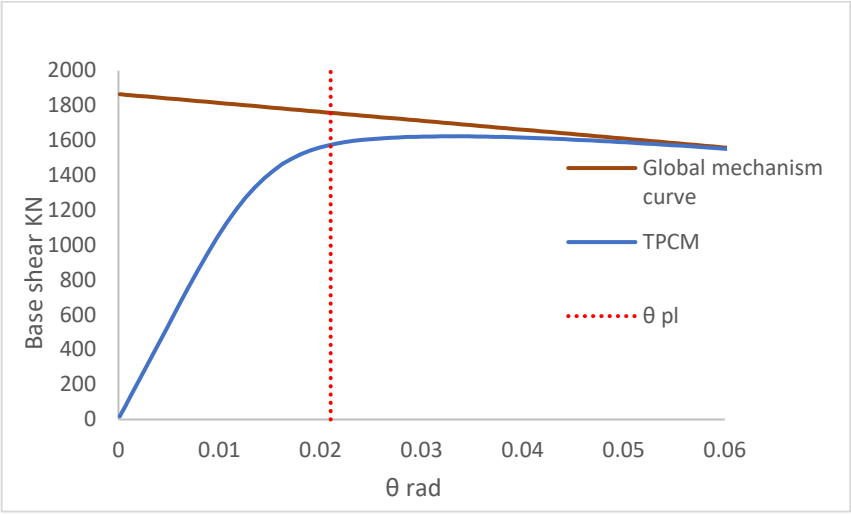

Figure 7.4 Push over curve TPM

8. CONCLUSIONS

Efficient and up-to-date standards and formulations are needed to make structures safe, sustainable and economical. This is especially true for stainless steel structures, given the high initial cost of raw materials and production. Thanks to the research work carried out over the years by many researchers, including the UPC group, nowadays there are current standards for designing stainless steel structures under static loads.

However, despite the potential of stainless steel in seismic design due to its ductility and strain hardening qualities, among others, there is not enough research on the behaviour and design of stainless steel structures under seismic conditions. Due to the lack of research, the next version of Eurocode 8, in charge of regulating seismic design, will not include its own specifications for stainless steel structures, although it will include them for aluminium.

In this context, the aim of this study is to evaluate the design rules proposed in the new version of Eurocode 8 for carbon steel in the design of stainless steel structures. For this purpose, a parametric study of multistorey moment resisting frames (MRFs) has been carried out covering three types of stainless steel: austenitic, ferritic and duplex. The designs of the frames (plans, elevations, vertical loads, seismic actions, masses and profiles) have been adopted from carbon steel S355 MRFs and DC2 ductility conditions studied by Lemma et al. (2022).

Stainless steel MRFs have been verified according to the new verifications for DC2 performing the force-based approach, which is the most common design method and is based on reducing the seismic action by a tabulated behaviour factor that depends on the material and the system.

It has been observed that all stainless steel frames have complied with the stability requirements, second order effect limitations and strength checks proposed by Eurocode 8. This is a consequence of a non-optimised design, i.e., for the same loads, the beam and column cross-sections should be smaller in stainless steel than in carbon steel. That is because the design remains in the elastic range and stainless steel exhibited a lower initial stiffness and higher yield strength values than carbon steel.

To assess the real behaviour factor, pushover analyses have been performed. It has been observed that the values of the global behaviour factor are much higher than the values proposed for carbon steel MRFs by Eurocode 8. This is the consequence of a non-optimised design. In addition, it was observed that duplex stainless steel exhibited the highest behaviour factor values because this alloy is quite ductile and has a high strain hardening, but the design remains in the elastic range, so the difference between the ultimate strength and design strength is remarkable.

Finally, the frames were designed following the Theory of Plastic Mechanism Control, which guarantees the global collapse mechanism. The profiles were found to be larger than those proposed by Lemma et al. (2022), which, however, as Abaqus shows, favor a global collapse mechanism. So in this specific case study the TPMC oversizes the profiles.

This study is intended to be a starting point in the proper calibration of the behaviour factor for stainless steel structures. As future research, it is recommended to increase the sample of frames analysed using more optimised profiles and thus obtain more realistic values of the q factor in DC2.

9. REFERENCES

ABAQUS, ABAQUS/Standard User's Manual Volumes I-III and ABAQUS CAE Manual, Dassault Systemes Simulia Corporation, 2016.

Afshan S., Zhao O., Gardner L. Standardised material properties for numerical parametric studies of stainless steel structures and buckling curves for tubular columns. *Journal of Constructional Steel Research* 2019; 152: 2–11.

Arrayago I., Rasmussen K.J.R., Real E. Statistical analysis of the material, geometrical and imperfection characteristics of structural stainless steels and members. Journal of Constructional Steel Research 2020; 175: 106378.

European Committee for Standardization (CEN). prEN 1993. Eurocode 3: Design of Steel Structures. Brussels, Belgium, 2021.

European Committee for Standardization (CEN). prEN 1993-1-4. Eurocode 3: Design of Steel Structures – Part 1-4: General Rules. Supplementary Rules for Stainless Steels. Brussels, Belgium, 2021.

European Committee for Standardization (CEN). prEN 1998-1-1. Eurocode 8: Design of structures for earthquake resistance – Part 1-1: General rules and seismic actions. Brussels, Belgium, 2021.

European Committee for Standardization (CEN). prEN 1998-1-2. Eurocode 8: Design of structures for earthquake resistance – Part 1-2: Rules for new buildings. Brussels, Belgium, 2021.

Gardner, L. and Ashraf, M. Structural design for non-linear metallic materials. Engineering Structures 2006, 5, Vol. 28, No. 6, pp. 926-934.

Hill, H.N. Determination of stress-strain relations from" offset" yield strength values. Washington, D.C., USA: National Advisory Committee for Aeronautics, 1944.

Mirambell, E. and Real, E. On the calculation of deflections in structural stainless steel beams: an experimental and numerical investigation. Journal of Constructional Steel Research 2000, 4, Vol. 54, No. 1, pp. 109-133.

Lemma M.S., Rebelo C., Silva L.S. da. Eurocode 8 revision - Implications on the design and performance of steel moment-resisting frames: Case study. *Soil Dynamics and Earthquake Engineering* 2022; 161: 107411.

Ramberg, W. and Osgood, W.R. Description of stress-strain curves by three parameters. Washington, D.C., USA: National Advisory Committee for Aeronautics, 1943.

Rasmussen, K.J.R. Full-range stress-strain curves for stainless steel alloys. Journal of Constructional Steel Research 2003, 1, Vol. 59, No. 1, pp. 47-61.

Steel Construction Institute (SCI). Design Manual for Structural Stainless Steel, 4th Edition. 2017.

V. Piluso, R. Montuori, E. Nastri. (2022). Theory of plastic mechanism control: A new approach for the optimization of seismic resistant steel frames. Fisciano, Salerno, Italia: Wiley.